Tritiation of stainless steel and cement particles enhances their genotoxic potential

Rebecca Castel, Alice Mentana, Virginie Tassistro, Cecilia Riani, Mickaël Payet, Olivier Debellemanière, Giorgio Baiocco, Elodie Bernard, Léa Plantureux, Stéphane Robert, et al.

Ecotoxicology and Environmental Safety 307 (2025) 119491

Contents lists available at ScienceDirect

Ecotoxicology and Environmental Safety

journal homepage: www.elsevier.com/locate/ecoenv

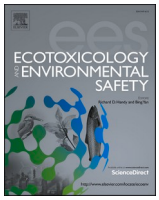

Tritiation of stainless steel and cement particles enhances their genotoxic potential

Rebecca Castel [a], Alice Mentana [c], Virginie Tassistro [a], Cecilia Riani [c], Mickaël Payet [b], Olivier Debellemanière [b], Giorgio Baiocco [c], Elodie Bernard [b], Léa Plantureux [e], Stéphane Robert [e], Véronique Malard [d], Thierry Orsière [a,*]

[a] Aix Marseille Univ., Avignon Univ., CNRS, IRD, IMBE, Marseille F-13005, France
[b] CEA, IRFM, Saint Paul lez Durance, F-13108, France
[c] Laboratory of Radiation Biophysics and Radiobiology, Department of Physics, University of Pavia, Pavia 27100, Italy
[d] Aix Marseille Univ., CEA, CNRS, BIAM, IPM, Saint Paul-Lez-Durance, F-13108, France
[e] AMUTICYT, Aix Marseille Univ., INSERM, INRAE, C2VN, UFR de Pharmacie, Marseille, France

ARTICLE INFO

Edited by Yong Liang.

Keywords:
Genotoxicity
Oxidative stress
THP-1 macrophages
Tritium
Cement particles
Steel particles

ABSTRACT

Tritium is a byproduct of nuclear fission activities and permeates in building materials. Decommissioning nuclear power plants could release tritiated steel and cement particles in the environment that could be accidentally inhaled by workers in case of loss of containment. Although tritium is a low energy beta emitter, tritiated particles could remain for years in the lungs after inhalation and subject them to long-term beta radiation. The aim of this study was to advance knowledge in the field of the radiotoxicity of these tritiated particles on human alveolar macrophages, capable of phagocytizing these particles. Although no cytotoxicity was observed, exposure to steel particles induced a significant increase in the production of reactive oxygen species (ROS), whereas exposure to cement particles induced a slight increase of ROS. Despite inducing high oxidative stress, control hydrogenated steel particles did not induce any DNA damage. Control hydrogenated cement particles also induced little DNA damage. DNA damage was higher after particle tritiation. The tritiation led to larger fractions of cells with similar levels of DNA damage, particularly at the lowest concentration. Significant chromosomal damage occurred after exposure to hydrogenated and tritiated particles, but only tritiated particles induced a concentration-dependent response. Overall, our results suggest that hydrogenated particles are moderately genotoxic and the tritiation of the same particles enhances their genotoxic potential, especially increasing their clastogenic potential. The data highlight a specific toxicity of tritiated particles on alveolar macrophages and improves the current knowledge of tritiated particles.

1. Introduction

Tritium is a radioactive isotope of hydrogen with a half-life of 12.3 years. It emits beta particles with a mean energy of 5.7 keV and a track length of 0.56 μm in water. It occurs naturally in the atmosphere due to cosmic rays and is rapidly converted to tritiated water (HTO). Concerning artificial sources, it comes essentially from nuclear facilities. It is produced in nuclear reactors as a byproduct of fission reactions at an estimated level of 0.1 EBq/year (UNSCEAR, 2017). As Europe is moving away from nuclear fission technology towards other types of energy, especially nuclear fusion technology, the increasing generation of nuclear energy world-wide and the renewal of old nuclear power plants, the risk of tritium release in the environment has increased. As an isotope of hydrogen, tritium has the same physical properties as hydrogen. It readily permeates through porous substances and can also diffuse in metal, thus contaminating the building materials of nuclear power plants. The move away from nuclear fission technology means that former nuclear power plants are being dismantled or will be in the coming years. Dismantlement operations generate micrometric and submicrometric tritiated particles of cement and steel, as both are found in reinforced concrete and steel can also be found in the pipework of nuclear power plants. The knowledge concerning their biological effects are still scarce. Despite safeguarding policies, there is a risk of exposure for workers and the local population in the event of a containment loss.

* Corresponding author.
E-mail address: thierry.orsiere@imbe.fr (T. Orsière).

https://doi.org/10.1016/j.ecoenv.2025.119491
Received 10 June 2025; Received in revised form 25 November 2025; Accepted 26 November 2025
Available online 28 November 2025

These particles can be inhaled and deposited in the respiratory tract, thus the workers and the local population may accidentally inhale tritiated particles. Although the European TRANSAT project did give some answers in terms of dosimetry, radiotoxicology, ecotoxicology and the environmental fate of tritiated cement and stainless steel particles (https://transat-h2020.eu), there is still a lack of data that the TITANS project (https://titans-project.eu/) aims to address.

The emitted beta particle alone does not have enough energy to penetrate the outer layer of the skin (Hill and Johnson, 1993). However, tritium can be inhaled, ingested and absorbed through the skin. Once in the organism, tritium can form HTO that behaves similarly to water. It is estimated that its biological half-life is of 10 days on average, like H_2O. Tritium can also be incorporated into organic molecules, thus forming organically bound tritium (OBT). OBT can remain in the organism for longer periods of time, from 40 days to a year, depending on the turnover rate of the tritiated organic molecules (Matsumoto et al., 2021). In this case, the cumulative radiation dose increases, resulting in higher cellular damage. In the case of inhalation of tritiated particles at the workplace, these particles could remain in the lungs for even longer periods of time. The pulmonary tissues would then be exposed to both particle-related stress and the beta-radiation of the tritium if tritium remains bound or partly bound to insoluble particles. Some dissolution of the particles may occur in the lungs and a fraction of its tritium content would be absorbed as HTO. For the insoluble tritiated particles, they could be removed from the lungs by mucociliary clearance and eliminated from the organism by the gastrointestinal tract or be phagocytized by macrophages (UNSCEAR, 2017). The main role of these cells of the immune system is to eliminate all organic debris and particles (Aderem and Underhill, 1999). Since alveolar macrophages can remain for years in the lungs, the radiation dose to these cells could be higher than expected (Patel et al., 2021). Exposure to the particles themselves is a health risk for workers in itself, especially for cement particles as it was already associated with an increased risk of laryngeal cancer for construction workers (Dietz et al., 2004). For stainless-steel particles, the exposure by inhalation is considered of low toxicity (Santonen et al., 2010); yet exposure to orthodontic appliances made in stainless steel did induce some genomic instability in buccal cells after 30 days (Westphalen et al., 2008).

Particulate and radiative stress both induce genetic damages that eventually lead to cancer (Sia et al., 2020; Turner et al., 2011). To better understand the genotoxic mechanisms underlying the possible toxicity of tritiated particles when inhaled, different in vitro toxicological studies can be performed. Oxidative stress is one of the possible actors of genetic instability (Dizdaroglu and Jaruga, 2012) and it can be assessed by quantifying the antioxidant defense of the cells or by assessing the reactive oxygen species produced after exposure. Studies usually focus on only one aspect of oxidative stress. The micronucleus assay (OECD, 2023) and the γH2AX assay have both been widely used as they are simple and sensitive tools to assess chromosomal losses and breakages as well as DNA strand breaks in any cells. The γH2AX assay's main advantage is its specificity to assess DNA damage only and the micronucleus assay is a well-established technique, with an OECD guideline (OECD, 2023) and is also used in biomonitoring chromosome damage after a radiation incident (Sari-Minodier et al., 2002, 2007; Wang et al., 2019).

A couple studies have evaluated the cyto-genotoxicity of tritiated particles, with either tungsten particles, stainless steel particles or cement particles (Lamartiniere et al., 2022; Uboldi et al., 2019). In each study, the cytogenetic effects of the tritiated particles were more severe than their hydrogenated counterparts, suggesting that tritium plays a key role in the enhanced genotoxicity of these particles (Baiocco et al., 2020; Mentana et al., 2022). Yet both studies were performed with BEAS-2B cells, which are epithelial cells. No studies have been performed on alveolar macrophages despite the fact that these cells are capable of phagocytosis and represent the first line of defense in an exposure scenario to tritiated particles. Thus, studying the effects of tritiated cement and stainless-steel particles on alveolar macrophages is necessary to assess all the health risks associated with exposure to these particles.

In this study, we used THP-1 monocytes that can be differentiated into macrophages for the different assays. We investigated the cytotoxicity, the genotoxicity as well as the oxidative stress after exposure to tritiated stainless steel particles and cement particles. The used particles mimic particles emitted during decommissioning operations. To discriminate between the effects of the particles and the radiative effects due to tritium, all assays were performed with hydrogenated particles and with tritiated particles. The localization of the particles was also assessed by imaging flow cytometry.

2. Methods

2.1. Reagents and products

HEPES, dihydrorhodamine-123, 40–6-Diamidino-2-phenylindole (DAPI), goat antihuman Alexa Fluor®488, fetal bovine serum (FS), Dulbecco's PBS 1X and penicillin-streptomycin antibiotics were provided by Life Technologies (Saint Aubin, France). Paraformaldehyde was provided by EMS (Hatfield, PA, USA). Bovine serum albumin fraction V was from Eurobio Scientific (Les Ullis, France). The antibody CD11b was provided by Biolegend (Amsterdam, The Netherlands). ProLong™ Gold antifade mountant, primary γ-H2AX antibody, goat normal serum and goat anti-rabbit secondary antibody coupled to an Alexa Fluor®488 were provided by OZYME (Saint-Cyr-L'École, France). All the other chemical products were provided by Sigma Aldrich (Lyon, France).

2.2. Cell culture and differentiation

THP-1 cells were isolated from peripheral blood from an acute monocytic leukemia patient (Cytion, Eppelheim, Germany). THP-1 cells are monocytes that can be differentiated into macrophages with 12-myristate 13-acetate phorbol (PMA) and have been used previously to study the toxicity of different types of particles (Butler et al., 2015; Longhin et al., 2013; McCarrick et al., 2021; Rakkestad et al., 2010).

THP-1 cells were cultured in RPMI 1640 medium (Cytion, Eppelheim, Germany) supplemented with 5 % FBS, 1 % penicillin-streptomycin antibiotics and 0.4 ‰ β mercaptoethanol. To differentiate THP-1 monocytes into macrophages, cells were seeded in the wellplates with medium containing PMA at a concentration of 0.2 μM and at a density of $1.10^5/cm^2$. The cells were left to differentiate for 72 h before the start of the experiments.

2.3. Cell exposure to particles

Particles were prepared similarly to the previous TRANSAT project. (Lamartiniere et al., 2022). Particles suspensions were prepared extemporaneously at a concentration of 5000 μg/ml. Stainless steel particles (SS316L) were suspended in 10 mM HEPES. Cement particles (CP) were suspended directly in the RPMI 1640 medium. For both types of particles, dilutions were performed in the medium to reach the chosen concentrations, ranging from 0 to 200 μg/ml. Cells were treated for 2 or 24 h, except the micronucleus assay where cells were treated for 48 h, according to the OECD 487 guideline (OECD, 2023). This assay require an exposure of 1.5–2 cell cycles, and THP-1 cells had a cell cycle averaging 45 h in our lab.

When cells were exposed to tritiated particles, tritiated water (HTO) was added as a second control to the assays. The activity used for HTO was equivalent to the highest activity of the particles (100 kBq/ml for SS316L particles and 6 or 12 kBq/ml for cement particles).

Cells were also exposed to hydrogenated particles to determine the toxicity due to the chemical and physical stress of particles and the toxicity due to both chemical and physical and radiative stresses.

2.4. Quantification of elemental and tritium release from particles

Particle stability was determined over a 24h-period by measuring the release of metals in suspensions of 100 μg/ml of hydrogenated stainless-steel particles and of 200 μg/ml of hydrogenated cement particles prepared in cell culture medium and incubated at 37°C. Two aliquots of each suspension were collected at 0 h, 0.5 h, 1 h, 2 h, 4 h, 8 h and 24 h for both types of particles. One aliquot was used to quantify Fe, Cr and Ni for stainless steel particles and Ca and Al for cement particles. Therefore, this sample was mineralized with aqua regia (3 v/1 v HCl: HNO3) for 24 h. For stainless steel particles, the second aliquot was centrifuged at 1635 g for 10 min to separate soluble and particle fractions in order to quantify the elemental release in the supernatant. For cement particles, the second aliquot was centrifuged at 11,000 g for 30 min then filtrated at 0.22 μm to obtain the soluble fraction and the pellet. The particles deposited on the filter could not be recovered. All the supernatants and the pellets samples were mineralized with aqua regia (3 v/1 v HCl: HNO3) for 24 h. Analysis was performed using an inductively couple plasma-mass spectrometry (ICP-MS, NexION® 300 X, PerkinElmer, MA, USA).

Tritium release was also evaluated over a 24h-period in suspensions of 100 μg/ml of tritiated stainless-steel particles and of 200 μg/ml of tritiated cement particles prepared in cell culture medium and kept at 37°C. The supernatants and pellets samples were obtained by applying the same protocol as described above. Analysis was performed by liquid scintillation counting (Tri-Carb 2910TR analyzer, Perkin Elmer, MA, USA).

2.5. Quantification of particle internalization by image flow cytometry

To study particle internalization by flow cytometry, THP-1 cells were differentiated in 6-wellplates at a density of 1.10^6 cells/well as described above. Cells were then exposed to increased concentrations of hydrogenated particles (0.05, 0.1,1,10, 25, 50 and 100 μg/ml). After 24 h of exposure to particles, cells were rinsed and trypsinized for 15 min before being scraped. Cells were put in 2 ml tubes to be centrifuged. Then cells were fixed with paraformaldehyde at 0.5 % for 10 min. Membranes were stained with CD11b-APC antibody at 10 μg/ml for 10 min and nuclei were stained with DAPI at 0.2 μg/ml for 10 min. Finally, cells were washed in PBS and cells were suspended in 40 μL of PBS. Analysis was performed with the Amnis® ImageStream®X (ISX) Mk II imaging flow cytometer. As this flow cytometry took images of each cell thanks to the imaging capacities of the ISX, we used the bright detail intensity (BDI) parameter feature provided on the side scatter channel (06). This parameter measured the variation of intensity on 7 pixels inside cells, reflecting a cell texture change in the side scatter, associated to particles internalization and allowed us to determine particle internalization. Cells that were not exposed to particles were used as a negative control to determine the limit of positivity value for BDI R7. To calculate BDI R7 on cells, the Intensity mask 06 was setup on a range between 2000 pixels and 4095 pixels (the maximum sensitivity of the camera). The results are expressed as the percentage of cells with a positive BDI on 7 pixels (% BDI R7 positive cells). For each experimental point, five independent assays were performed.

2.6. Cell viability assay

Cell viability was assessed using the XTT assay by following the protocol of the supplier Xenometrix (Allschwill, Switzerland). This colorimetric in vitro assay is based on the reduction of XTT to formazan, an orange compound, by mitochondrial dehydrogenase viable cells. To perform this assay, cells were differentiated in 96-well plates. After 72 h, the medium was removed, and the cells were rinsed with PBS. Cells were exposed to increasing concentrations of hydrogenated and tritiated particles of stainless steel and cement, from 0.1 μg/ml to 200 μg/ml. Exposure durations were 2 h and 24 h. The negative controls were 5 % HEPES buffer for SS316L and medium for CP. The positive control was 10 % Triton X-100. The cytotoxicity of tritiated water (HTO) was also assessed in similar conditions, with activities ranging from 0.005 kBq/ml to 200 kBq/ml, activities observed for tritiated particles.

After exposure, cells were rinsed with PBS and 100 μL of fresh medium along with 25 μL of the XTT reagent were added in each well. Cells were incubated at 37°C, 5 % CO2 for 3 h. Analyses were performed with a spectrophotometer MultiSkan (ThermoScientific) or a Spectra Max M5 Microplate reader (Molecular Devices, San Jose, CA, USA) at 480 nm and 690 nm. Data analysis was carried out by first substracting the optic density measured at 690 nm to the optic density measured at 480 nm for each well, then Eq. 1 was applied. Two independent assays were performed, each assay performed in two plates with three-wells per condition.

$$\%inhbition = 100 - \left(\frac{\overline{DO}_{condition} - \overline{DO}_{blanks}}{\overline{DO}_{negative} - \overline{DO}_{blank}} \times 100 \right) \quad (1)$$

2.7. Oxidative stress

2.7.1. Reactive oxygen species kinetic measurement

Dihydrorhodamine-123 (DHR-123) is a compound that oxidizes into rhodamine 123 in presence of intracellular H2O2. To assess the oxidative stress with this compound, cells were differentiated in black 96-well plates. The medium was removed, and the cells were rinsed with PBS. Cells were then incubated with dihydrorhodamine-123 in PBS diluted to 1/1000th for 45 min at 37°C, 5 % CO2. Cells were exposed to increasing concentrations of hydrogenated and tritiated particles of stainless steel (SS316L) and cement (CP), from 1 μg/ml to 100 μg/ml. Positive controls were H2O2 at 500 μM and at 1 mM. Negative controls were 5 % HEPES buffer for SS316L and medium for CP. All the exposure solutions were added in another black 96-wellplate without any cells to determine if the particles can oxidize DHR-123. Measurements of the fluorescence were done after 0.5 h, 1 h, 2 h, 4 h, 8 h and 24 h of exposure. All the plates were incubated at 37°C, 5 % CO2 before analysis with a fluorescence plate reader POLARstar (Omega) or a Spectra Max M5 Microplate reader (Molecular Devices, San Jose, CA, USA) with λ excitation of 485 nm and λ emission at 520 nm. Results are expressed as an increase of the fluorescence based on the average fluorescence of the negative control.

2.7.2. Antioxidant defense

The antioxidant defense of the cells was assessed by quantifying the oxidized (GSSG) and the total (GSSG+GSH) glutathione in cultured cells by using the GSH/GSSG-Glo™ Assay (Promega, Charbonnières-les-Bains, France), a luminescence-based assay. The luminescent signal is proportional to the amount of GSH in the cells, and a reduction of the ratio indicates that cells were in an oxidative environment.

According to the manufacturer's instructions, THP-1 cells were differentiated in opaque 96-wellplates. Cells were exposed to suspensions of tritiated particles of 1, 5, 10,50 and 100 μg/ml for 2 h, a time based on the oxidative stress kinetic study. Two activities of HTO were also assessed (100 kBq/ml for SS316L and 12 kBq/ml for cement particles). After exposure, cells were lysed. Luciferin detection reagent was added, and plates were incubated for 15 min before analysis of the luminescence by the Spectra Max M5 Microplate reader (Molecular Devices, San Jose, CA, USA). Data were analysed by subtracting the

GSSG reaction signal from the total glutathione to obtain the value of reduced glutathione (Eq. 2).

$$\frac{GSH}{GSSG}ratio(condition) = \frac{Luminescence\ total\ glutathione - Luminescence\ GSSG}{Luminescence\ GSSG/2} \quad (2)$$

The assay was performed twice independently.

2.8. Genotoxicity assays

2.8.1. DNA damage

2.8.1.1. H2AX assay. The phosphorylation of the histone H2AX is considered as marker of DNA damage since this process is essential to recognize and repair DNA strand breaks (Watters et al., 2009). This phosphorylation can be assessed by immunofluorescence.

Briefly, THP-1 cells were differentiated at in LabTek™ 4-well chamber slides (LabTeck™ II Nalgene Nunc International, Villebon-sur-Yvette, France). The medium was removed, and the cells were rinsed with PBS. Cells were exposed to increasing concentrations of hydrogenated and tritiated particles of SS316L and cement, from 1 μg/ml to 100 μg/ml, during 2 h and 24 h. Positive control was H2O2 at 125 μM. The negative control was 2.5 % HEPES buffer. After exposure, cells were rinsed and fixed with paraformaldehyde at 4 % for 10 min at ambient temperature. Then cells were permeabilized with a mixture of 0.5 % Triton-X 100, 2 % bovine serum albumin (BSA) and PBS for 10 min at ambient temperature. Nonspecific sites were blocked with a blocking buffer (PBS/5 % Normal Serum/0.3 % Triton X-100) for 30 min at ambient temperature. Cells were then incubated with the primary antibody γ-H2AX (diluted to 1/550th) in the antibody dilution buffer (PBS/ 1 % BSA / 0.5 % Triton X-100) overnight at 4°C in the dark. Afterwards, cells were incubated with the Goat Anti-Rabbit secondary antibody coupled to an Alexa Fluor®488 probe diluted at 1/600th in the antibody dilution buffer for 1 h at ambient temperature in the dark. Finally, cells were incubated with DAPI diluted to 0.2 μg/ml in PBS for 10 min at ambient temperature in the dark. Once the staining finished, cells were rinsed, the chambers were removed, slides were mounted using Prolong™ Gold antifade reagent. All slides were kept at 4°C until analysis.

The fluorescence microscope was either a Zeiss Axio Imager A.2 (Zeiss SAS, Marly le Roi, France) with a filter combination, a Nikon camera (Melville, New York, NY, USA) and the NIS-Elements software or a Zeiss Axio Imager Z2 with a CoolCube 4 camera by Metasystems and the corresponding Metafer™ v4.3.5 software (Metasystems, Althlussheim, Germany).

We used the Fiji software (v. 2.15.1) to measure the intensity of 100 nuclei per slide and of the background fluorescence to correct for the background intensity. Data was then used to determine the corrected total cell fluorescence (CTCF) (Eq. 3).

$$CTCF = \text{int}\ egrated\ density - (cell\ area \times background\ mean\ fluorescence) \quad (3)$$

2.8.1.2. Data treatment for inhomogenous exposure scenario. Due to the highly inhomogeneous exposure scenario, a large fraction of cells remains undamaged. To properly account for this aspect in the experimental data interpretation, a further analysis of CTCF data was performed following the approach proposed in Mentana et al., (2023). Considering the full distribution of the radiobiological endpoint, here the CTCF for the γH2AX signal, rather than its average value as done standardly, such approach allows to evaluate the fraction of damaged cells and the average damage level in these cells separately.

We considered as experimental conditions the 24-hour exposures to hydrogenated or tritiated stainless steel and cement particles or HTO, at all the concentrations tested.

Starting from the distribution of cell nuclei scored with different CTCF values for a single condition, histograms with the number of cells scored in CTCF bins with a width of 100000 (arbitrary units) were created. Cells with CTCF < 350000, corresponding to about 80 % of the total in the control condition (C-), were considered undamaged and all histograms were normalized setting to 1 their number.

The data treatment then proceeded following the steps reported in Material and Methods in Mentana et al. (Mentana et al., 2023). In particular, for a specific exposure condition (test) and the corresponding control condition (ctrl), we calculated the distribution of the quantity □ (arbitrary units, proportional to the number of cells) vs CTCF (Eq. 4) which corresponds to the distribution of the extra damaged cells at different CTCF levels with respect to the control population.

$$\delta(test) = \#cell(test) - \#cell(ctrl) \quad (4)$$

From the vs CTCF distributions, we are able to calculate two quantities (Eq. 5):

$$\Delta \quad (test) = \sum\nolimits_{CTCF} \delta(test) \quad (5)$$

proportional to the number of damaged cells (obtained summing up all the □ values over all CTCF bins) for a single exposure condition, and the average value of the □ distribution (Eq. 6):

$$< CTCF >_{\delta} \quad (test) = \frac{1}{\Delta}\sum\nolimits_{CTCF} \delta \bullet CTCF \quad (6)$$

proportional to the average level of DNA damage in damaged cells only for a single exposure condition. These two quantities are finally interpreted as a function of particle concentrations. As an example, the treatment is illustrated for a chosen condition in all its steps in Fig. SI 1 (Supplementary Information).

2.8.2. Chromosomal damage

To assess chromosomal breakage and chromosome loss following particles exposure, the micronucleus assay with centromere labelling was performed in compliance with the OECD 487 guideline (OECD, 2023).

Briefly, THP-1 cells were seeded in 12-wellplates at a density of 1.10^6 cells/well and treated with increasing concentrations of particles for 48 h. Cells were counted to calculate the Relative Population Doubling (RPD) (Eq. 7), then cells were recovered in 2 ml-tubes to be centrifuged and rinsed with PBS.

$$RPD = \frac{Number\ of\ population\ doubling\ in\ treated\ cultures}{Number\ of\ population\ doubling\ in\ control\ cultures} \times 100 \quad (7)$$

where

$$population\ doubling = \log(post\ treatment\ cell\ number \div initial\ cell\ number) \div \log 2$$

Cells were fixed with 4 % PFA. After permeabilization with 2 % BSA/ 0.05 % Triton-X 100, the centromere labelling was performed by successively incubating the cells with CREST antibody (diluted 1/1000th)

and Alexa Fluor®488 anti-human antibody (diluted 1/500th). Then the cytoskeleton was stained with 0.06 μg/ml of Phalloidin-TRITC for 30 min, and the nuclei was stained with DAPI at 0.2 μg/ml for 10 min. Finally, cells were suspended in 100 μL of Prolong™ Gold antifade and 50 μL of this suspension was smeared on a slide. This step was repeated twice to have two slides per experimental point and the micronucleus assay was performed in independent duplicates.

Analysis was done by using a fluorescence Zeiss Axio Imager A2 microscope or an Olympus BX60 microscope at 600x magnification. Micronuclei were assessed in 500 cells/slide, with an overall of 4 slides and 2000 cells per condition.

2.8.3. PCA analysis

Starting from the large dataset obtained for different endpoints, an integrated analysis has been conducted with a principal component analysis (PCA) approach. This technique allows a data dimensionality reduction, mapping high-dimensional data into a two-dimensional space, and allows to find and highlight possible patterns enhancing differences among tested conditions. The starting points are defined by coordinates representing the following set of variables: cell viability; ROS production; the Δ and <CTCF> quantities (as defined respectively in Eqs. 5 and 6 from γ-H2AX analysis); relative population doublings; chromosomal damage, measured as fold-increase of micronucleated cells (for C+MN, C-MN and MultiMN). We included in the analysis the set of variables corresponding to: the control condition (unexposed cells); cells exposed for 24 h at three different chosen concentrations of hydrogenated SS316L and CP particles (1 μg/ml, 10 μg/ml and 100 μg/ml) and at the corresponding activity levels in case of tritiated particles (1 kBq/ml, 10 kBq/ml and 100 kBq/ml for steel, and 0.06 kBq/ml, 0.6 k Bq/ml and 6 k Bq/ml for cement); cells exposed for 24 h to HTO, at the two tested activity levels (12 and 100 kBq/ml). PCA was applied after standard feature scaling to avoid bias due to the integration of variables with largely varying numerical values.

2.8.4. Statistical analysis

Statistical analysis was performed with GraphPad Prism (v10.3.1). Normality tests and equal variance were done to determine if an ordinary one-way ANOVA, a Welch ANOVA or an equivalent non-parametric test should be applied. Then a post-hoc test was applied, either a Dunnett's or a Dunn's multiple comparisons test. For the micronucleus assay, a chi-squared test was applied to the data.

3. Results

3.1. Elemental and tritium release in the cell culture medium

Elemental and tritium release were assessed after preparing hydrogenated and tritiated particle suspensions that incubated at 37°C and that were sampled at different time points up to 24 h. Measurements were done by ICP-MS for SS316L particles, by ICP-OES for cement particles and by liquid scintillation counting to assess tritium release.

SS316L particles released little amounts of elements: nearly 10 % of Fe and Mn were released in the medium and less than 1 % for Cr, Ni and Mo during the 24 h of the experiments (Fig. SI 2). Cement particles had higher dissolution rates, as about 56 % of Al and 36 % of Ca were released in the medium over the course of the experiment (Fig. SI 2).

Most of the tritium remained in the particles for SS316L particles and only a little was released in the medium (< 10 %) (Fig. 1). For cement particles, the opposite was observed: most tritium was released in the medium and less than 30 % remained in the particles (Fig. 1).

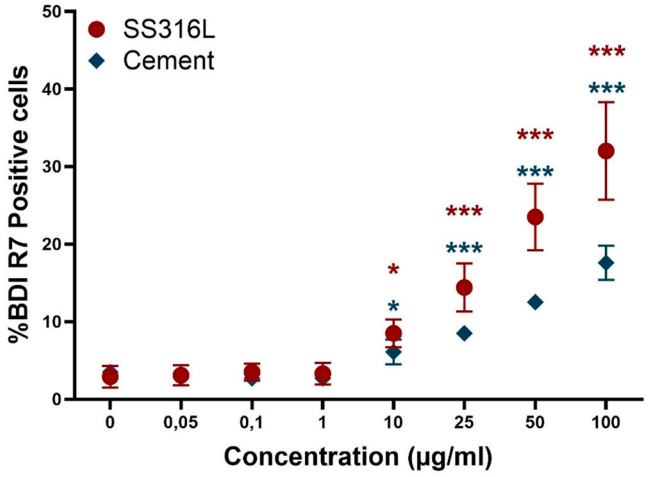

Fig. 2. Internalization of hydrogenated SS316L and cement particles in differentiated THP-1 macrophages, measured by imaging flow cytometry. * p-value < 0.05, *** p-value < 0.001.

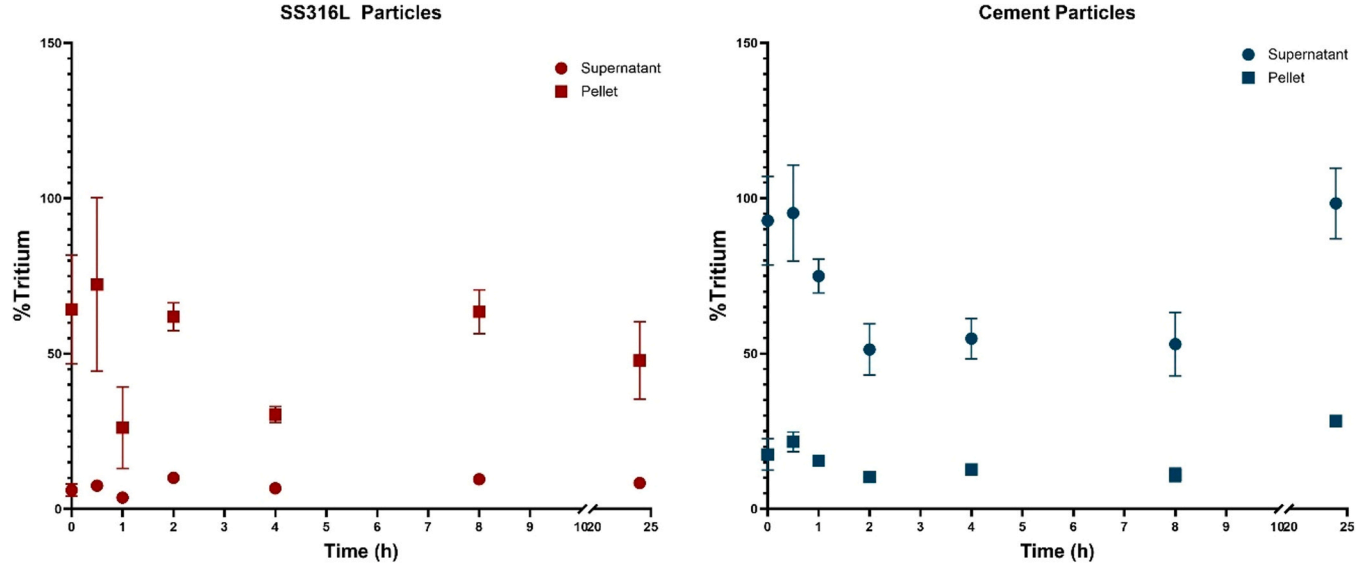

Fig. 1. Percentage of tritium in the supernatants and in the pellets of the particle suspensions in cell culture medium. The tritiated SS316L particle suspensions were at 100 μg/ml and the tritiated cement particle suspensions were at 200 μg/ml. The suspensions were incubated at 37°C and samples were collected at different time points. The tritium amount was measured via liquid scintillation counting. Data are presented as the mean ± SEM of three independent experiments.

3.2. Particle internalization by flow cytometry

Particle internalization by THP-1 cells differentiated into macrophages was measured by flow cytometry, by using the side scatter channel. Cells with a positive variation in bright detail intensity on 7 pixels (%BDI R7 positive cells) were considered as cells having internalized particles.

Below 10 μg/ml, no increase in positive cells was observed (Fig. 2). However, the increase is significant starting from 10 μg/ml for both types of particles and the significance increases at 25 μg/ml. For cement particles, there were fewer positive cells than for SS316L particles. This could be due to the fact cement particles tend to be smaller (about 1.7 μm on average vs 2.6 μm for SS316L particles) hence are less detected than SS316L particles and that they are more soluble than SS316L (Rose et al., 2019).

3.3. Cell viability

Cell viability was investigated after exposure of differentiated THP-1 human macrophages up to 200 μg/ml of hydrogenated and tritiated particles.

When cells were exposed to SS316L particles for 2 h, only one condition reduced significantly cell viability: we observed 61.5 % of cell viability when cells were exposed to 200 μg/ml of hydrogenated SS316L

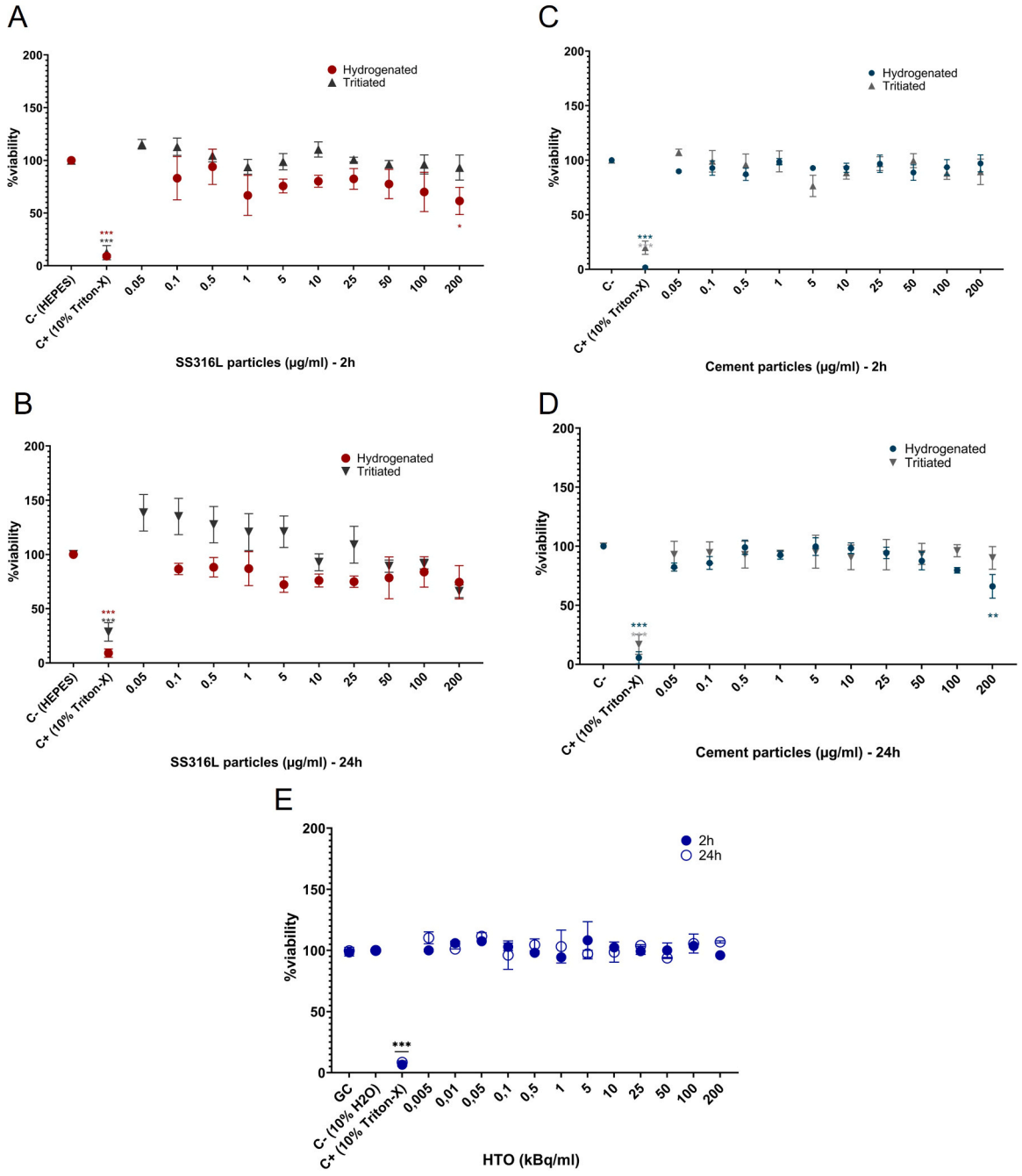

Fig. 3. Cytotoxicity of hydrogenated and tritiated particles measured after 2 h and 24h-exposures in differentiated THP-1 cells. The tritiated SS316L particles had an increasing radioactivity of 0.05,0.1,0.5,1,5,10,25,50,100 and 200 kBq/ml. The tritiated cement particles had an increasing radioactivity of 0.003,0.006,0.03,0.06,0.3,0.6,1.5,3,6,12 kBq/ml. Data are presented as mean ± SEM of two independent experiments, each in duplicate and three wells/condition (n = 12). Statistical significance was tested by a Kruskal-Wallis test and a post-hoc Dunn's multiple comparison test with * $p < 0.05$, ** $p < 0.01$, *** $p < 0.001$.

(Fig. 3A). At 24 h, there was no inhibition when cells were exposed to hydrogenated or tritiated SS316L particles (Fig. 3B).

When cells were exposed to hydrogenated and tritiated cement particles for 2 h, there was no reduction in cell viability (Fig. 3C). After 24 h, tritiated cement particles did not reduce cell viability (Fig. 3D); however, hydrogenated particles did decrease cell viability at 200 μg/ml (66.1 % viability).

Overall, tritiated particles induced little to no inhibition, regardless of the type of particles and of the exposure concentrations. Likewise, exposure to tritiated water did not inhibit cell viability (Fig. 3E).

3.4. Oxidative stress

3.4.1. Reactive oxygen species kinetic measurement

As oxidative stress is a main factor leading to DNA damage (Dizdaroglu and Jaruga, 2012), we investigated the ability of particles to generate reactive oxygen species in THP-1 cells. The ROS production was measured the fluorescence of rhodamine, a product of the oxidation of dihydrorhodamine-123 by ROS. Results pertaining to the exposure of THP-1 macrophages to SS316L particles are presented in Table 1 whereas results pertaining to the exposure to cement particles are presented in Table 2.

Hydrogenated SS316L particles induced a significant increase of fluorescence after 30 min (5–10.9 %), 1 h (4.6–11.5 %) and 4 h (5.1–48.7 %) of exposure at each concentration (Table 1). After 2 h of exposure, only 100 μg/ml of particles induced a significant increase of fluorescence (10.1 %). After 8 h of exposure, the 3 highest concentrations induced a significant increase of fluorescence (19.2–81.3 %) and after 24 h, most concentrations (except 1 μg/ml) induced a significant increase in fluorescence (29.4–151.2 %). Overall, the oxidation of DHR-123 into rhodamine increased with time and with the concentration of SS316L in the medium (Table 1).

After 30 min of exposure, no concentration of tritiated SS316L induced an increase in fluorescence. However, all the concentrations induced a significant increase in fluorescence after 1 h and 2 h of exposure (22.2–30.3 % and 16.2–31.6 % respectively). The highest concentration (100 μg/ml) induced a significant increase in fluorescence after 4 h, 8 h and 24 h of exposure (48.1 %, 47.3 % and 57.1 % respectively). Only one other condition, 1 μg/ml after 8 h, induced a significant increase (37.4 %) (Table 1).

Interestingly, the measured values of tritiated SS316L were higher than the values of hydrogenated SS316L. After 30 min, the increases ranged from 27.2 % to 41.4 % compared to 5–10.9 %; after 1 h, 22.2–30.3 % compared to 4.6–11.5 %; after 2 h, 16.2–31.6 % compared to −1.01–10.1 %. It's only after 4 h of exposure that the fluorescence was comparable between the two groups (-0.8–48.1 % for tritiated particles and 5.11–48.8 %). After 8 h and 24 h, hydrogenated particles induced a higher increase in ROS production than tritiated particles (0.23–81.33 % and 20.5–151.1 % compared to 11.6–47.3 % and 7,62–57.1 % respectively) (Table 1). Tritiated SS316L seems to induce more oxidative stress quickly after exposure (<4 h) whereas hydrogenated particles seem to induce more oxidative stress after a longer exposure (>4 h).

Hydrogenated cement particles induced a small but significant increase of fluorescence after 30 min of exposure at 1 μg/ml and 5 μg/ml (1.5 % and 1.7 % respectively) (Table 2). A small increase was also observed after 2 h of exposure to 5 μg/ml (2.3 %). After 24 h of exposure, a small but significant increase was observed for most conditions except 5 μg/ml, with an increase ranging from 3.2 % to 4.1 %. Overall, the increases were small (<5 %) and the oxidation of DHR was mostly time dependent.

Tritiated cement particles also induced small increases in fluorescence, from −0.6–9.8 % after 30 min of exposure to −1.8–28.5 % after 24 h of exposure. Only two conditions were significant: the exposure to 1 μg/ml for 8 h (17.3 %) and the exposure to 100 μg/ml for 24 h (28.5 %) (Table 2).

Table 1
Kinetic ROS production measured by fluorescence of rhodamine-123 in THP-1 cells differentiated in macrophages upon exposure to hydrogenated and tritiated SS316L particles. Each value represents the mean increase in fluorescence normalized on the negative control ± SEM of two independent experiments. The p-value was assessed after a post-hoc comparison test (Dunett's or Dunn's depending on the normality of the data) and p-values < 0.05 are in bold.

	Time (h)															
	0,5 h			**1 h**			**2 h**			**4 h**			**8 h**			**24 h**		
SS316L	**Mean**	**SEM**	***p-value***	**Mean**	**SEM**	***p-value***	**Mean**	**SEM**	***p-value***	**Mean**	**SEM**	***p-value***	**Mean**	**SEM**	***p-value***	**Mean**	**SEM**	***p-value***
Hydrogenated																		
C-	0	0,68		0	0,61		0	0,30		0	1,01		0	0,76		0	1,56	
1 μg/ml	10,93	0,33	*0,0943*	11,15	0,38	***< 0,0001***	1,68	0,40	*0,6267*	15,57	0,47	*0,0943*	1,95	0,60	*0,9972*	20,49	3,75	*0,0943*
5 μg/ml	5,28	0,24	***0,0051***	5,86	0,27	***0,0008***	0,99	1,35	*0,9562*	5,11	0,65	***0,0051***	0,23	1,78	*> 0,9999*	29,44	4,57	***0,0051***
10 μg/ml	6,88	1,03	***0,0041***	6,16	0,28	***0,0004***	-1,01	0,63	*0,9515*	18,92	1,02	***0,0041***	19,23	4,00	***< 0,0001***	30,02	3,00	***0,0041***
50 μg/ml	7,82	0,72	***< 0,0001***	7,28	0,36	***< 0,0001***	4,13	0,85	*0,0561*	31,21	0,93	***< 0,0001***	31,94	1,46	***< 0,0001***	136,04	5,63	***< 0,0001***
100 μg/ml	5,00	0,31	***< 0,0001***	4,62	0,26	***0,0124***	10,15	1,03	***< 0,0001***	48,77	2,27	***< 0,0001***	81,33	6,54	***< 0,0001***	151,21	14,77	***< 0,0001***
C+ (500 μM H2O2)	14,39	2,61	*0,9434*	14,50	2,62	***< 0,0001***	10,53	1,39	***< 0,0001***	10,96	1,17	*0,9434*	6,65	0,53	*0,4282*	7,43	1,88	*0,9434*
C+ (1 mM H2O2)	11,56	0,40	*0,7965*	14,08	1,36	***< 0,0001***	13,20	1,14	***< 0,0001***	15,30	1,22	*0,7965*	9,45	1,09	*0,0915*	9,94	1,39	*0,7965*
Tritiated																		
C-	0	3197		0	2,12		0	2,95		0	1,58		0	2518		0	2,98	
1 kBq/ml	27,19	5821	*0,7099*	30,26	5,29	***0,0035***	16,17	3,76	***0,0352***	-0,764	10,55	*> 0,9999*	37,37	12,58	*0,0204*	7,62	6,69	*> 0,9999*
5 kBq/ml	35,24	10,6	*0,484*	27,18	5,84	***0,0125***	24,44	5,14	***0,0122***	12,572	7,83	*> 0,9999*	18,32	6039	*0,9545*	10,18	8,90	*> 0,9999*
10 kBq/ml	41,39	8484	*0,6457*	26,64	5,80	***0,0136***	28,28	5,15	***0,0043***	25,065	10,12	*> 0,9999*	11,63	5327	*> 0,9999*	27,31	6,51	*0,7981*
50 kBq/ml	32,72	6,25	*0,3301*	22,21	2,95	***0,0003***	21,92	3,83	***0,0042***	32,042	8,37	*0,157*	29,51	3012	*0,0507*	37,29	2,38	*0,1354*
100 kBq/ml	30,35	5452	*0,1295*	25,39	2,89	***< 0,0001***	31,59	2,18	***< 0,0001***	48,151	5,89	***0,012***	47,28	6616	***0,0025***	57,06	2,29	***0,0008***
C+ (HTO) 100 kBq/ml	4,66	2175	*0,8581*	27,87	1,75	***< 0,0001***	12,17	2,99	*0,074*	6846	3,79	*> 0,9999*	2,62	1742	*> 0,9999*	-5,88	8,70	*> 0,9999*
C+ (1 mM H2O2)	-13,68	10,68	*0,8485*	-2,21	10,01	*0,8241*	72,76	12,03	***0,0002***	15,519	7,24	*> 0,9999*	9,18	7327	*> 0,9999*	9,28	7,62	*> 0,9999*

Table 2
Kinetic ROS production mtaeasured by fluorescence of rhodamine-123 in THP-1 cells differentiated in macrophages upon exposure to hydrogenated and tritiated cement particles. Each value represents the mean increase in fluorescence normalized on the negative control ± SEM of two independent experiments. The p-value was assessed after a post-hoc comparison test (Dunett's or Dunn's depending on the normality of the data) and p-values < 0.05 are in bold.

	Time (h)															
	0,5 h			**1 h**			**2 h**			**4 h**			**8 h**			**24 h**		
Cement	**Mean**	**SEM**	***p-value***	**Mean**	**SEM**	***p-value***	**Mean**	**SEM**	***p-value***	**Mean**	**SEM**	***p-value***	**Mean**	**SEM**	***p-value***	**Mean**	**SEM**	***p-value***
Hydrogenated																		
C-	0	0,34		0	0,57		0	0,55		0	0,29		0	0,20		0	1,06	
1 µg/ml	1,79	0,54	*0,0489*	0,09	0,36	*> 0,9999*	1,48	0,41	*0,1596*	0,06	0,38	*> 0,9999*	0,29	0,20	*0,9998*	3,22	1,11	***0,0141***
5 µg/ml	1,93	0,37	***0,0284***	-0,49	0,30	*0,9164*	2,49	0,68	*0,0034*	-0,22	0,42	*0,9993*	0,92	0,25	*0,8771*	2,72	0,59	*0,0521*
10 µg/ml	0,81	0,57	*0,7166*	-0,26	0,25	*0,997*	1,06	0,26	*0,4805*	0,04	0,23	*> 0,9999*	-0,09	0,49	*> 0,9999*	3,28	0,39	***0,0121***
50 µg/ml	0,51	0,20	*0,9539*	-1,11	0,22	*0,2297*	1,12	0,43	*0,4167*	-0,08	0,24	*> 0,9999*	-0,77	0,43	*0,9453*	3,95	0,45	***0,0016***
100 µg/ml	-0,92	0,35	*0,5925*	-0,64	0,22	*0,7608*	0,92	0,22	*0,6212*	-1,13	0,11	*0,2634*	-0,56	0,43	*0,9895*	4,09	0,31	***0,0015***
C+ (500 µM H2O2)	5,63	0,74	***< 0,0001***	3,71	0,57	***< 0,0001***	6,83	0,48	***< 0,0001***	4,63	0,57	***< 0,0001***	8,12	0,27	***< 0,0001***	11,30	0,73	***< 0,0001***
C+ (1 mM H2O2)	6,09	0,57	***< 0,0001***	5,63	0,56	***< 0,0001***	7,18	0,71	***< 0,0001***	9,62	0,86	***< 0,0001***	13,62	1,88	***< 0,0001***	14,42	0,70	***< 0,0001***
Tritiated																		
C-	0	1,17		0	2,26		0	3,25		0	2,59		0	2,90		0	2,56	
1 kBq/ml	-0,60	1,14	*> 0,9999*	4,38	2,86	*> 0,9999*	4,39	2,46	*> 0,9999*	27,78	11,96	*0,3093*	17,35	4,96	***0,0261***	-1,83	2,6	*> 0,9999*
5 kBq/ml	-0,42	1,64	*> 0,9999*	-2,73	0,71	*> 0,9999*	-1,29	2,83	*> 0,9999*	0,88	4,55	*> 0,9999*	5,83	8,08	*> 0,9999*	-3,92	3,08	*> 0,9999*
10 kBq/ml	-0,03	0,82	*> 0,9999*	8,93	3,1	*0,4308*	7,59	5,28	*> 0,9999*	6,29	4,79	*> 0,9999*	1,03	4,46	*> 0,9999*	5,30	3,53	*> 0,9999*
50 kBq/ml	3,97	4,22	*> 0,9999*	-1,44	2,04	*> 0,9999*	4,31	3,72	*> 0,9999*	-1,11	5,16	*> 0,9999*	-6,48	2,53	*> 0,9999*	21,81	7,96	*0,2401*
100 kBq/ml	9,84	3,43	*0,2429*	7,47	2,69	*0,7349*	-0,53	1,72	*> 0,9999*	14,49	5,45	*0,5853*	14,98	9,74	*0,2886*	28,54	7,89	***0,0495***
C+ (HTO) 100 kBq/ml	7,84	2,00	*0,0736*	10,33	5,02	*0,6094*	-2,01	3,38	*> 0,9999*	4,79	6,77	*> 0,9999*	5,13	3,91	*> 0,9999*	8,45	3,16	*> 0,9999*
C+ (1 mM H2O2)	-21,09	6,56	*0,7639*	-13,00	6,19	*> 0,9999*	54,00	14,99	***0,013***	-49,94	3,56	***0,0007***	-0,02	10,95	*> 0,9999*	28,12	16,6	*> 0,9999*

Finally, it is worth highlighting that HTO did not increase significantly the oxidation of DHR-123 at 12 kBq/ml and at 100 kBq/ml except for one condition (cells exposed to 100 kBq/ml for 1 h).

3.4.2. Antioxidant defense

The GSH/GSSG ratio was assessed by GSH/GSSG-Glo™ Assay. It is a luminescence-based assay, and it was performed only with tritiated particles. The exposure was 2 h long.

For SS316L particles (Fig. SI 3 A), no significant decrease was observed for the positive control for both independent experiments. Therefore, the assay was considered inconclusive. For cement particles (Fig. SI 3B), there was a significant decrease of the GSH/GSSG ratio for the positive control (20 µM menadione) and a slight decrease for HTO. The ratio did not decrease when cells were exposed to tritiated cement particles. Thus, the exposure to cement particles had no impact on the antioxidant defense of THP-1 macrophages.

3.5. Genotoxicity assays

3.5.1. DNA damage – H2AX results

DNA damage was assessed by the γH2AX assay. The fluorescence intensity of the γH2AX foci in the nuclei were measured, then we calculated the CTCF (Eq. 3) to correct for the background intensity. Average CTCF values for all the cell nuclei were first analyzed.

Following exposure to hydrogenated SS316L particles for 2 h, there were no significant increase in DNA damage (Fig. 4A). After an exposure of 24 h, there was even a slight significant decrease in DNA damage at 10 and 50 µg/ml (Fig. 4B).

Following exposure to hydrogenated cement particles for 2 h, there was a significant increase in DNA damage at 50 µg/ml and 100 µg/ml (Fig. 4C). After an exposure of 24 h, only 100 µg/ml induced a significant increase in DNA damage (Fig. 4D).

Following exposure to tritiated SS316L particles for 2 h, each condition induced a significant increase in DNA damage, including exposure to HTO. However, the response was not concentration-dependent. The lowest concentrations, 1 and 5 µg/ml, induced the most DNA damage and 10 µg/ml induced the least (Fig. 4A). After an exposure of 24 h, we observed similar results: each condition induced a significant increase in DNA damage, with 1 and 5 µg/ml inducing the most DNA damage and 50 µg/ml inducing the least (Fig. 4B).

Following exposure to tritiated cement particles for 2 h, there were significant increases in DNA damage at each experimental point. Similarly to tritiated SS316L, the lowest concentrations (1 and 5 µg/ml) induced the most DNA damage whereas 10 µg/ml induced the least (Fig. 4C). After an exposure of 24 h, there was a significant increase in DNA damage at each endpoint. Once again, the lowest concentrations (1 and 5 µg/ml) induced the most DNA damage and 10 µg/ml induced the least (Fig. 4D).

HTO on its own induced a significant increase in DNA damage at 100 kBq/ml whereas at 6 kBq/ml, it only induced a significant increase after 24 h of exposure (Fig. 4). Overall, the tritiation of the particles seems to enhance their genotoxic potential, as we observed higher levels of DNA damage with tritiated particles than with hydrogenated particles when γH2AX signals are averaged on the cell population.

3.5.2. DNA damage – distribution / inhomogenous exposure

To properly consider the inhomogeneous exposure scenario in the genotoxicity evaluation, a further CTCF data analysis was performed, considering the full distribution of nuclei scored at different CTCF levels. Results of this analysis, in terms of □ (Eq. 5) and <CTCF> (Eq. 6), are shown in Fig. 5 for cells exposed, for 24 h, to stainless steel particles (top panels) and cement particles (bottom panels) as a function of particle concentration. In both cases, the comparison between hydrogenated (in blue) and tritiated (in red) particle exposure shows how the presence of tritium leads to an increase in the number of damaged cells (□), especially at low concentration (up to 10 □g/ml), without increasing the

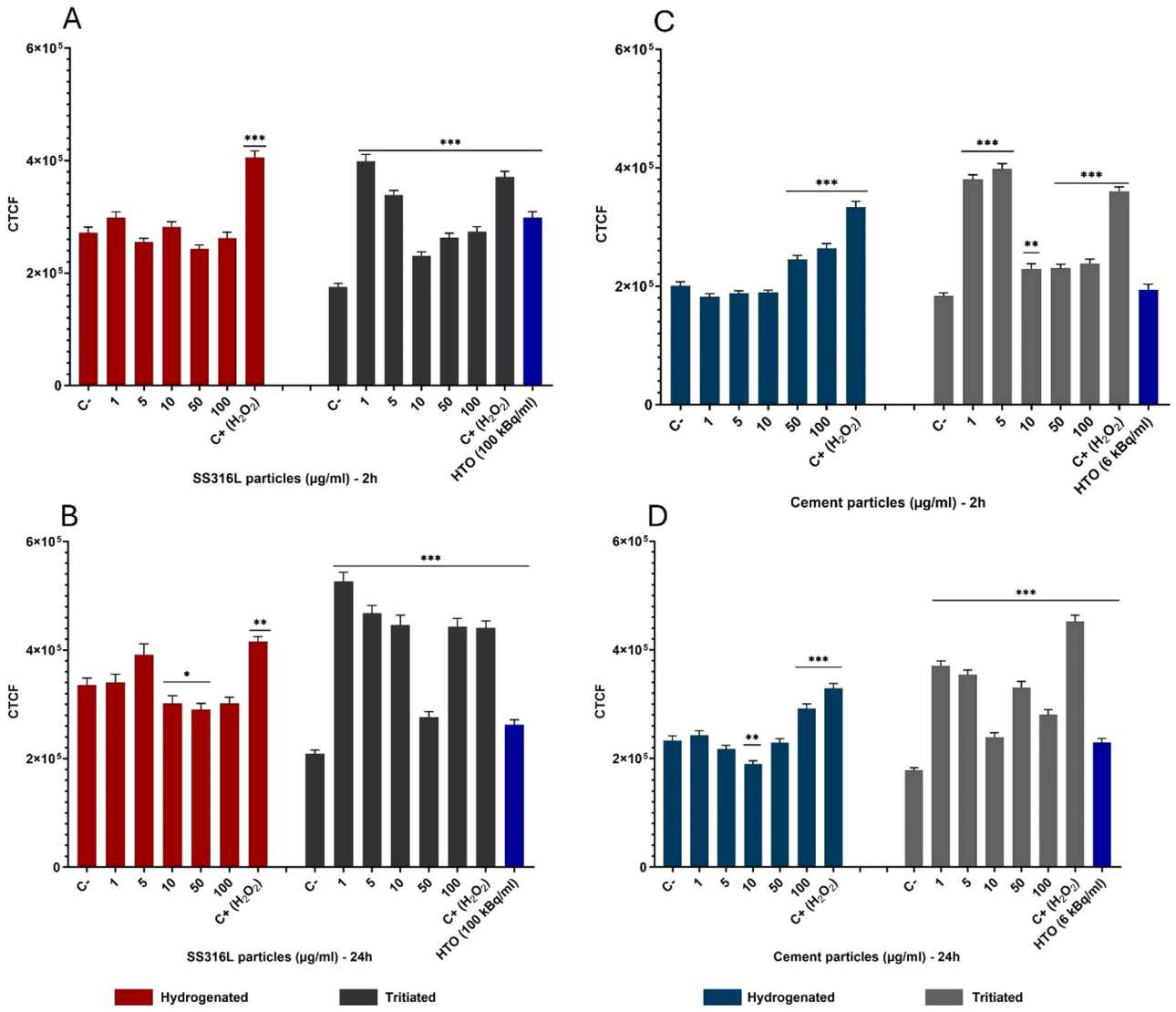

Fig. 4. DNA damage was measured by the phosphorylation of H2AX in differentiated THP-1 cells, following an exposure to SS316L and cement particles. The tritiated SS316L particles had an increasing radioactivity of 1,5,10,50 and 100 kBq/ml. The tritiated cement particles had an increasing radioactivity of 0.06,0.3,0.6,3 and 6 kBq/ml. Data are presented as a mean ± SEM of two independent experiments, each in duplicate. * p-value < 0.05; ** p-value < 0.01; *** p-value < 0.001.

average damage level (<CTCF>), which remains fairly constant for damaged cells over all the particle concentrations. HTO seems not to increase the number of cells and the damage level.

3.6. Chromosomal damage

Chromosomal damage was assessed with a micronucleus assay. The types of micronuclei were discriminated by labelling the centromeres (C) of chromosomes with CREST. If the micronucleus (MN) was labelled positively (C+MN), then it was caused by the loss of a whole chromosome. If the MN was not labelled (C-MN), then it was caused by the breakage of the chromosome after a double strand break (OECD, 2023).

The doubling of the THP-1 monocytes was determined for each experiment (from 1.10^6 cells to at least 2.10^6 cells per condition). The RPD (Eq. 7) was then assessed. There was no significant decrease or increase in RPD for each condition (Fig. SI 4).

Following exposure to hydrogenated SS316L particles (Fig. 6A), each concentration induced a significant increase in micronuclei, with a significant increase of both C+MN and C-MN. The negative control had a base level of 28 micronuclei per 1000 cells. There was no dose dependent increase, the fold-increase in micronuclei was similar amongst the different concentrations.

Following exposure to hydrogenated cement particles (Fig. 5A), each concentration induced a significant increase in micronuclei. The negative control had a base level of 54 micronuclei per 1000 cells. All concentrations induced also a significant increase in C-MN. Except 5 µg/ml, there was also a significant increase in C+MN. The results were similar to the ones obtained with SS316L as there was no dose dependent fold-increase.

Following exposure to tritiated SS31L (Fig. 6B), there was a significant increase in micronuclei at each endpoint and the results were concentration-dependent. The negative control had a base level of 9 micronuclei per 1000 cells. The lowest concentration, 1 µg/ml, did not induce any significant increase in C-MN. There was also no significant induction of C+MN at 1,5 and 10 µg/ml. There was a significant increase of C-MN at 5 and 10 µg/ml. Only 50 and 100 µg/ml increased significantly both types of micronuclei.

Following exposure to tritiated cement particles (Fig. 6B), there was a significant increase in micronuclei at each endpoint. The negative control had a base level of 11 micronuclei per 1000 cells. Overall, the

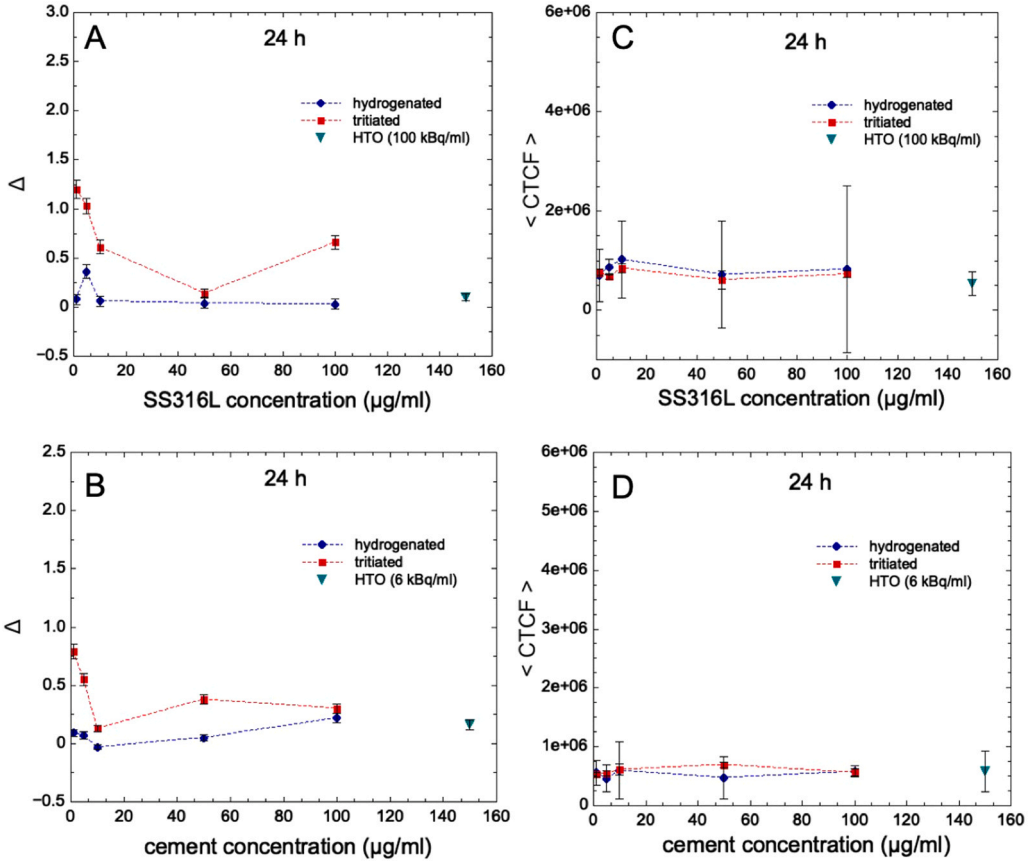

Fig. 5. Evaluation of the extra damaged cells (D) and their average DNA damage level (<CTCF>) with respect to the control population (unexposed cells), after 24 h of exposure to stainless steel and cement particles and HTO. A and C: D and <CTCF> in cells exposed to stainless steel hydrogenated (in blue) and tritiated (in red) particles at different concentrations and to 100 kBq/ml of HTO (in green). B and D: D and <CTCF> in cells exposed to cement hydrogenated (in blue) and tritiated (in red) particles at different concentrations and to 6 kBq/ml of HTO (in green). Error bars have been calculated using error propagation laws, starting from an error on each bin of the d distribution of the square root of number of counts.

results are similar to the ones obtained with tritiated SS316L. The lowest concentration, 1 µg/ml, did not significantly induce C+MN and C-MN. There was also no significant induction of C+MN at 5 µg/ml but there was a significant increase in C-MN. The other three concentrations (10, 50 and 100 µg/ml) increased significantly both types of micronuclei.

Following exposure to HTO (Fig. 6B), there was a significant increase in micronuclei when THP-1 monocytes were exposed to 100 kBq/ml HTO but not to 12 kBq/ml HTO.

Overall, the different concentrations of hydrogenated particles induced the same level of micronuclei. The tritiation of these particles seems to increase their genotoxic potential as there was a concentration-dependent/activity-dependent increase in micronuclei when THP-1 monocytes were exposed to tritiated particles and tritiated water.

3.7. PCA analysis results

Results of the PCA analysis are reported in Fig. 7. The analysis captures a clear discrimination among conditions, with a visible clustering of points corresponding to cells exposed to hydrogenated particles (circles), separated from the control and from those corresponding to cells exposed to tritiated particles (squares). Points corresponding to cells exposed to HTO ideally belongs to the same half-plane of all samples with tritium activity from particles. A color-based discrimination (CP, in green vs. SS316L particles, in orange) can also be guessed, though with a less striking pattern. Overall, no net concentration effect is visible (symbol size is proportional to particle concentration), but the two conditions corresponding to the highest concentration/activity level for hydrogenated/tritiated SS316L particles show the maximal distance in the PC1 vs. PC2 space from the clusters they ideally belong to.

4. Discussion

To assess the hazard of particulate matter generated by the decommissioning of nuclear power plants, the toxicity of tritiated stainless steel particles and cement particles was investigated using in vitro assays. Hydrogenated particles were also used to determine the toxicity due to the chemical and physical stress.

During dismantlement, in the event of a containment accident, workers may be exposed to tritiated particles by inhalation. The TRANSAT project thus assessed the in vitro toxicity of tritiated particles and HTO on human lung epithelial cells (Baiocco et al., 2020; Lamartiniere et al., 2022; Mentana et al., 2022, 2023). However, the main target of such particles in the lungs would be macrophages as their main role is to eliminate debris and particles (Berte et al., 2021). The THP-1 cell line is a common cell model used in in vitro toxicology studies since it is easy to handle and can be differentiated into macrophages.

Concerning stainless steel particles, a review on their toxicity concluded that these particles were likely to have little toxicity in humans (Santonen et al., 2010). Harmful toxic effects on humans have not been reported despite the countless uses of stainless steel over the past decades. In agreement with the literature, steel particles induced only a slight decrease in cell viability at 200 µg/ml (Badding et al., 2014; Cediel-Ulloa et al., 2021; Kodali et al., 2022; McCarrick et al., 2021).

Concerning exposure to Portland cement particles, studies show some evidence of a possible adverse effect of these particles on the respiratory tract and of a potential carcinogenicity (Adeyanju and

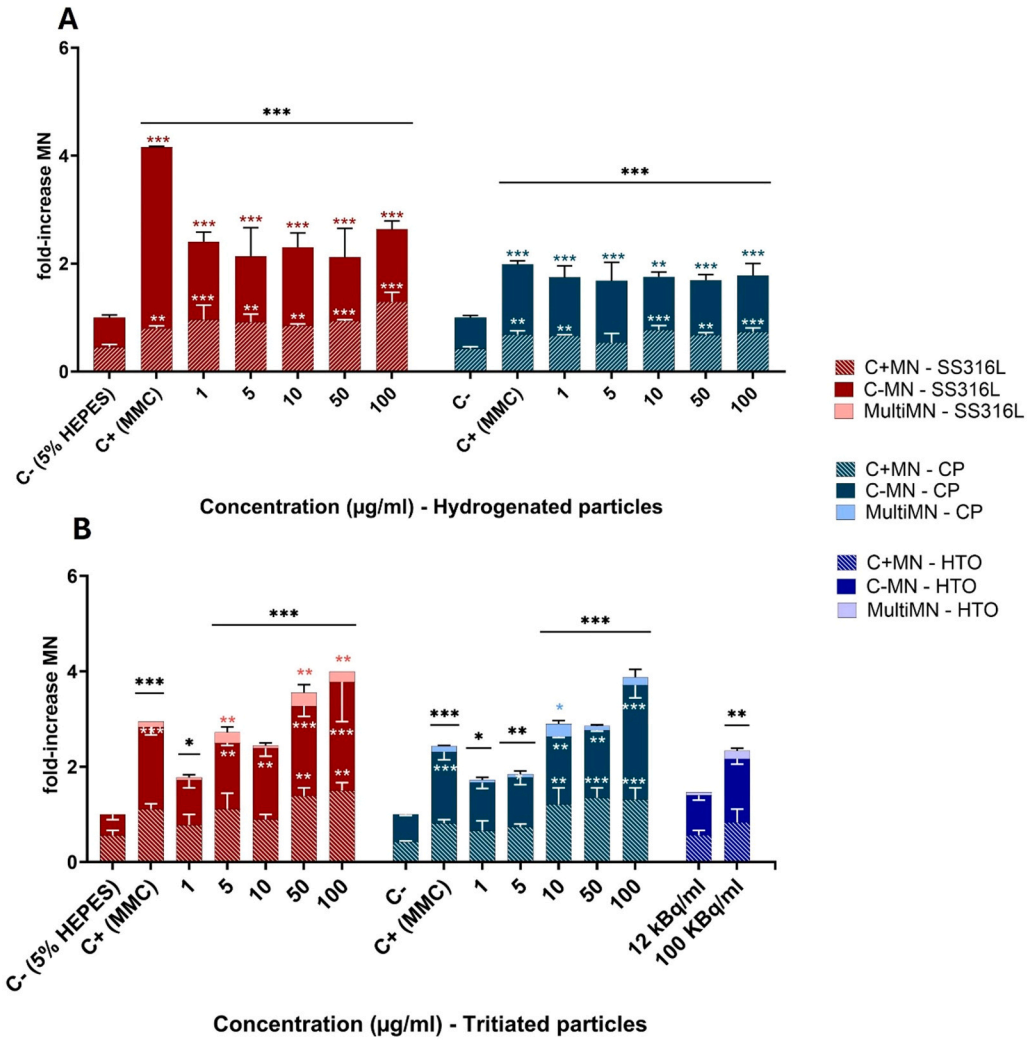

Fig. 6. Chromosomal damage assessed by the micronucleus assay performed on THP-1 cells, after exposure to SS316L and cement particles for 2 cell-cycles. Centromere (C) labelling with Crest was performed to discriminate between micronuclei issued by whole chromosome loss (C+MN) and MN resulting from chromosome breakage cause by double strand break (C-MN). The tritiated SS316L particles had an increasing radioactivity of 1,5,10,50 and 100 kBq/ml. The tritiated cement particles had an increasing radioactivity of 0.06,0.3,0.6,3 and 6 kBq/ml. Data are represented as means ± SEM of two independent experiments. Statistical significance was assessed by a χ-squared test. * p-value < 0.05; ** p-value < 0.01; *** p-value < 0.001.

Okeke, 2019; Fell and Nordby, 2017; Hartwig and MAK Commission, 2022; Raffetti et al., 2019). In agreement with the literature on the in vitro effects of Portland cement particles, there was only a significant decrease in cell viability at 200 µg/ml induced by cement particles (Bauer et al., 2010; Lamartiniere et al., 2022; Sgambato et al., 2010; Van Berlo et al., 2009).

Oxidative stress is also an important endpoint to study since many contaminants, including particles and nanoparticles, may generate reactive oxygen species (ROS) that will target intracellular biomolecules, including lipids and DNA, causing lipid peroxidation and DNA damage (Dizdaroglu and Jaruga, 2012; Lee et al., 2012; Pandey and Prajapati, 2018). Moreover, stainless steel particles contain iron and chromium, both metallic elements that can generate ROS via Fenton-like reactions or Haber-Weiss reactions (Lee et al., 2012).

The ability of SS316L particles and cement particles to generate ROS was assessed by measuring the oxidation of DHR-123 by luminescence. SS316L particles, probably due to their high content in Fe and Cr, generated the most ROS whereas cement particles generated little to no ROS over the span of 24 h. Tritiated SS316L particles induced more ROS than hydrogenated SS316L particles before 4 h of exposure and hydrogenated SS316L particle induced more ROS than tritiated SS316L particles after 4 h of exposure. Tritiated cement particles did induce slightly more ROS than hydrogenated cement particles after 8 h.

Studies have shown that stainless steel particles do induce oxidative stress, in agreement with our own results (Badding et al., 2014; Cediel-Ulloa et al., 2021; Leonard et al., 2010). In the study by Cedial-Ulloa et al., they observed only a small increase in ROS production; it could be due to the use of a different cellular model (human small airway epithelial cells). Badding et al. and Leonard et al. have both used RAW 264.7 mouse macrophages. Badding et al. studied the ROS production over the course of 7 h after an exposure to 50 µg/ml to stainless-steel welding fumes. The response was significant after 2 h and continued to rise over the course of the 7 h (Badding et al., 2014). Leonard et al. studied the lipid peroxidation along with H2O2 production after an exposure to 250 µg/ml of stainless-steel welding fumes for 1 h and 30 min respectively. There was a significant increase in both lipid peroxidation and H2O2 production, it also highly increased after just 30 min (Leonard et al., 2010).

Concerning cement particles, papers have assessed the oxidative stress in different cellular models after exposure to cement particles or dust (Ogunbileje et al., 2014; Sgambato et al., 2010; Van Berlo et al., 2009). Ogunbileje et al. have studied the effect of different cement dusts on murine macrophages after a 12h-long exposure and have shown that there was a significant increase in ROS at 50 µg/ml for two types of

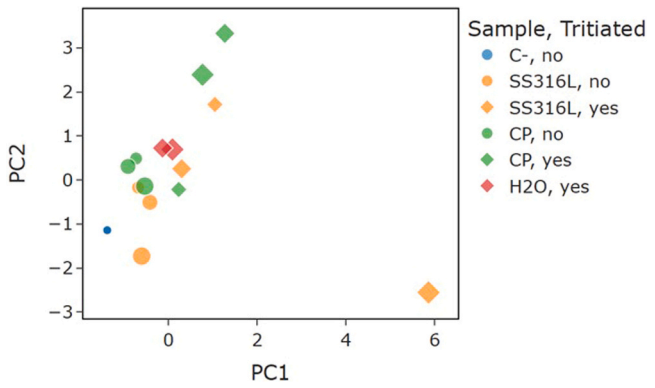

Fig. 7. Principal component analysis on data (cell viability; ROS; Δ and <CTCF>; relative population doublings; fold-increase in C+MN, C-MN and MultiMN) for: unexposed cells (C-, label: Tritiated, no); cells exposed for 24 h to 1 μg/ml, 10 μg/ml and 100 μg/ml of SS316L and CP (label: Tritiated, no) and to the corresponding activity levels in case of tritiated particles (1 kBq/ml, 10 kBq/ml and 100 kBq/ml for steel, and 0.06 kBq/ml, 0.6 k Bq/ml and 6 k Bq/ml for cement, label: Tritiated, yes); cells exposed for 24 h to HTO at the two tested activity levels (12 and 100 kBq/ml). PCA was applied after standard feature scaling. The marker size is concentration/activity dependent. PC1 and PC2 explain respectively 33.4 % and 25.2 % of the variance in the analyzed dataset.

cement dust (Nigerian and American) and a significant increase at 200 μg/ml for the last type of cement dust, produced from clinker. Van Berlo et al. also studied the effects of cement dusts on murine macrophages and observed no increase in ROS production after 3 h of exposure. Sgambato et al. studied the oxidative DNA damage with 8-OHdG in murine fibroblasts when exposed to Portland cement dust. They observed no oxidative DNA damage after 1 h and 24 h of exposure.

For tritium alone, Quan et al. studied the effect of HTO on epithelial cells (Quan et al., 2020). After an exposure of 5 h to 2 MBq/ml and a resting time of 19 h, they did not observe any significant increase in ROS production Our own results showed a significant increase at 100 kBq/ml after 1 h. The difference in methodology makes it hard to compare our two studies as we did not add a resting period for the cells before measuring the fluorescence. However, it would seem HTO does not induce ROS.

Overall, our results agree with the literature. Stainless steel particles seem to increase ROS production whereas findings for cement particles and dusts are more inconsistent. There is insufficient data on the oxidative stress generated by HTO. All of this highlights the need for further studies.

The antioxidant defense is another important endpoint to assess, as reduced glutathione plays a crucial role in protecting cells from oxidative stress. An alteration in ratio of reduced/oxidized forms of glutathione (GSH/GSSG) reveals that cells are subjected to oxidative stress.

Our own results were inconclusive for SS316L particles when the GSH/GSSG ratio was assessed in THP-1 macrophages. Very few studies have assessed the glutathione ratio after exposure to stainless steel particles. In a study on workers exposed to such particles, the antioxidant defense of the erythrocytes were in the normal ranges with no significant differences between a non-exposed group and the exposed workers (Mongiat et al., 1992). In a study on liver cells, the exposure to stainless steel nanoparticles barely decreased the GSH/GSSG ratio at 100 μg/ml after 24 h and 48 h (Almutairi et al., 2021). In the previous TRANSAT project, Lamartinière et al. also did not observe any alteration in the GSH/GSSG ratio on BEAS-2B cells after a 30 min exposure to SS316L particles. However, in a study on ultrafine stainless steel particles, the GSH/GSSG ratio was significantly altered after 4 h of exposure on BEAS-2B cells after an exposure to 1.5 μg/cm^2, indicating that the cells were subjected to oxidative stress (Boudjema et al., 2021). The literature is not conclusive on the effect of stainless-steel particles on the antioxidant defense and there is a need for further studies.

For cement particles, we observed no effect of the exposure on the GSH/GSSG in THP-1 macrophages after 2 h. Our results are in agreement with the ones obtained by Van Berlo et al. They did not observe any decrease in the glutathione levels after 4 h of exposure on murine macrophages (Van Berlo et al., 2009). Our results are also similar to the ones obtained by Lamartinière et al. during the TRANSAT project (Lamartiniere et al., 2022). They did not observe any alteration of the GSH/GSSG ratio on BEAS-2B cells after a 30 min exposure to cement particles. However, Ogunbileje et al. did observe a decrease in intracellular GSH at 50 μg/ml after 12 h on murine macrophages (Ogunbileje et al., 2014). Orman et al. also observed a decrease in GSH levels in erythrocytes of cement workers compared to the control-group.

Concerning the effect of tritium on the antioxidant defense, a study on mice has shown that there was no effect on the production of enzymes implicated in the antioxidant defense such as glutathione peroxidase (Kelsey-Wall et al., 2006).

Overall, there is not enough evidence on the effect of stainless-steel particles and cement particles on the GSH/GSSG ratio on different cellular models. Moreover, it is important to note that macrophages are more resistant to ROS as they constitute the immune system's first line of defense. (Bauer et al., 2010; Berte et al., 2021). Indeed, they can generate ROS depending on the phagocytosis mechanism (Aderem and Underhill, 1999).

The genotoxicity endpoint is of interest as the DNA damage and/or chromosomal damage are a key component to the pathological consequences of oxidative stress and ionizing irradiation (Sia et al., 2020).

The DNA damage was assessed by using the γH2AX assay as the phosphorylation of this histone is marker of a DNA breakage (Watters et al., 2009).

Our study showed some similarities in terms of DNA damage between the two types of particles. Hydrogenated SS316L particles did not induce any DNA damage after 2 h and 24 h of exposure. Hydrogenated cement particles induce a significant increase in DNA damage at 50 μg/ml and 100 μg/ml after 2 h and only at 100 μg/ml after 24 h. When particles were tritiated, we observed a higher increase in DNA damage when γH2AX signal was averaged over the whole cell population for 1 μg/ml and 5 μg/ml, no matter the exposure time and no matter the nature of the particle. HTO alone also increased DNA damage at 6 KBq/ml after 24 h and at 100 kBq/ml after 2h-exposure and 24h-exposure.

A further analysis of the results obtained for 24 h of exposure was performed adapting the approach originally proposed by Mentana et al. for comet data in case of inhomogeneous exposure (Mentana et al., 2023). The analysis revealed that, for both particle kinds, tritiation seems to increase the fraction of damaged cells, without increasing the average damage level when looking at these cells only. This knowledge highlights the possible implication of tritium in the promotion of carcinogenesis: a larger fraction of genetically damaged cells indicates a higher risk of genetic alteration and a possible initiation of carcinogenesis. This information could also improve risk assessments by taking into account the higher frequency of damaged cells after an exposure to tritiated particles.

Literature on the genotoxicity of stainless steel particles and cement particles agree on the fact that these particles can induce an increase in DNA damage (Badding et al., 2014; Leonard et al., 2010; Sgambato et al., 2010). Some studies even show a dose dependent response when cells are exposed to them (Lamartiniere et al., 2022; McCarrick et al., 2021; Ogunbileje et al., 2014). One study assessed in situ DNA fragmentation and observed an increase between 50 μg/ml and 200 μg/ml when cells were exposed to cement dust (Ogunbileje et al., 2014). However, one paper did not observe any DNA damage when A549 and BEAS 2B cells were exposed to steel particles (Kain et al., 2012), in agreement with our own results. The difference in results could be due to the use of different assays: they mostly all used the comet assay, which quantifies all types of DNA damage whereas the H2AX assay quantifies specifically DNA strand breaks.

For tritiated particles, Lamartinière et al. also observed a concentration-dependent increase in DNA damage averaged over the cell population when BEAS-2B cells were exposed to tritiated SS316L and cement particles (Lamartiniere et al., 2022). Also in that case, if data are analyzed following Mentana et al., 2023, the observed tritium-induced increase in DNA damage could be attributed to an increase of the fraction of damaged cells in the population, while the damage level for damaged cells only was found to be the same for exposure to hydrogenated or tritiated SS316L particles (Mentana et al., 2023). A couple other studies also found that human cells exposed to HTO had an increase in DNA damage (Cui et al., 2016; Quan et al., 2020).

Interestingly, in the previous TRANSAT project, which investigated the effects of the same particles, Rose et al. observed in the particle suspension the presence of quasi ultra fine (QUF) particles ranging from 0.21 to 1 μm for hydrogenated SS316L particles and also that the higher the concentration, the more particles aggregated (Rose et al., 2019). Dubey et al. observed the localization of atmospheric QUF (0.1–0.32 μm) particles compared to atmospheric fine (0.32 μm-1.8 μm) and atmospheric coarse (1.8–10 μm) particles sampled inside Chinese hamster lung fibroblasts (Dubey et al., 2022). Coarse and fine particles were uptaken by phagocytosis by the fibroblasts and were found near the periphery of the cells. QUF particles were uptaken by endocytosis and were found in vacuoles near the nuclei of the cells. The closer the tritiated QUF particles are to the DNA, the likelier the emitted β-particle could induce direct DNA damage as it has an average range of 0.5 μm. Studies have shown that QUF particles may also induce DNA damage and chromosomal damage (Boudjema et al., 2021; Panico et al., 2020; Platel et al., 2020). This genotoxicity could be due to an impairment of mitochondrial function and oxidative stress (Dubey et al., 2022; Loxham et al., 2015; Sotty et al., 2020). However, data on the genotoxicity of QUF particles is scarce and revolves around ambient air particles, with varying composition depending on the size of the particles (Steenhof et al., 2011).

Therefore, our hypothesis is that the tritiation of the QUF particles could render them genotoxic to macrophages at low levels of exposure that do not induce the aggregation of QUF particles. More research needs to be done on the potential formation of QUF particles in the suspensions of tritiated SS3316L particles and tritiated cement particles, on their uptake by macrophages and their localization inside the cells. Further characterization by means of image flow-cytometry measurements could help to gain insight on this, though a size limit in particle detection needs to be considered: indeed, the fraction of cells internalizing particles is increasing with particle concentration in our dataset for values above 10 μg/ml, but this does not exclude the internalization of QUF particles leading to the observed biological effects also below this concentration threshold.

In terms of chromosomal damage, it was assessed by the way of the micronucleus assay following the OECD 487 guideline (OECD, 2023). This assay was conducted using THP-1 monocytes since they are also capable of particle phagocytosis (Berte et al., 2021).

Both hydrogenated SS316L particles and cement particles induced the formation of clastogenic and aneugenic micronuclei. The response was not concentration-dependent in our study. Lamartinière et al. observed a similar phenomenon on BEAS-2B cells (Lamartiniere et al., 2022) whereas a study on the genotoxicity of Portland cement particles did find a concentration-dependent increase in micronuclei formation on epithelial cells (Pawliczak et al., 2021). In another study on the exposure of cement warehouse workers, the authors observed an increase in micronuclei formation the longer the workers were exposed to Portland cement dust (Krishna et al., 2020). It has been reported before that stainless steel can induce an increase in micronuclei (Westphalen et al., 2008), but there was no information regarding a concentration-dependent response.

For tritiated particles, the increase in micronuclei formation was concentration-dependent, with a bigger increase in the formation of clastogenic micronuclei. The tritiation of the particles enhanced their genotoxicity.

Our results are coherent with the study performed by Lamartinière et al., as they also observed an increase in micronuclei formation with tritiated particles (Lamartiniere et al., 2022). Mice exposed to tritiated water and organically-bound tritium did not show any significant increase in micronuclei in their bone marrow cells (Roch-Lefèvre et al., 2018), but fathead minnows did have an increase in micronuclei in their blood cells when exposed to tritiated water and organically-bound tritium (Gagnaire et al., 2020). Thus, we cannot exclude the contribution of tritium to the overall genotoxicity of these particles. Moreover, a study suggested that possible mechanisms of genotoxicity could be a direct interaction between the naked nuclear DNA during mitosis and/or a direct mechanical influence on the cytoskeleton, thus disturbing the mitotic spindle (Malkova et al., 2021).

If particles did interact directly with the DNA during mitosis, it could in part explain the increase in chromosomal damage sustained by the cells when they were exposed to increasing concentrations of tritiated particles.

5. Conclusion

The aim of this study was to assess the cytotoxicity, the oxidative stress and the genotoxicity of tritiated SS316L and Portland cement particles on the human THP-1 cells. This cell line was chosen as macrophages and monocytes are the target of particle exposure as they are capable of phagocytosis (Berte et al., 2021).

We found overall little cytotoxicity, both for hydrogenated and tritiated particles. In terms of oxidative stress, cement particles induced little ROS production, and there was no measured impact on the antioxidant defense. For SS316L particles, there was a big increase in ROS production over 24 h for both hydrogenated and tritiated particles. It is probably due to the high content in iron and chromium of these particles, that can lead to Fenton-like reactions or Haber-Weiss reactions. From a genotoxic standpoint, the hydrogenated particles induced little DNA damage whereas their tritiated counterpart induced some significant DNA damage. A detailed data analysis taking into account particle inhomogeneity suggests that tritiation increases the fraction of cells showing DNA damage, rather than the average damage level in damaged cells, especially at low particle concentration. Indeed, DNA damage was more evident when cells are exposed to the lowest concentrations: a hypothesis is the presence of tritiated quasi ultra fine particles that did not aggregated at lower concentrations and which were able to induce DNA damage due to a potential proximity to the nucleus. For chromosomal damage, the hydrogenated particles did significantly generated micronuclei, but the increase did not depend on the concentration. However, the tritiated particles did increase significantly the number of micronuclei, especially via a clastogenic mechanism, in a concentration-dependent way.

Our results show that the tritiation status of particles can enhance their genotoxic potential. As macrophages and monocytes are the main targets in case of accidental exposure to inhaled particles and macrophages can remain for years in the lungs, there is a need to further study the immunotoxicity and the long-term effects these particles could have. Moreover, there is a need to better characterize the smallest particles in the suspensions, their potential localization in the cells and their specific toxicity.

CRediT authorship contribution statement

Elodie Bernard: Project administration, Funding acquisition, Conceptualization. **Véronique Malard:** Writing – review & editing, Supervision, Project administration, Methodology, Conceptualization. **Giorgio Baiocco:** Writing – review & editing, Resources, Methodology. **Mickaël Payet:** Writing – review & editing, Resources, Methodology, Formal analysis. **Olivier Debellemanière:** Writing – review & editing,

Resources, Methodology, Formal analysis. **Virginie Tassistro:** Writing – review & editing, Visualization, Resources, Investigation, Formal analysis. **Cecilia Riani:** Writing – original draft, Visualization, Investigation, Formal analysis. **Léa Plantureux:** Writing – review & editing, Resources, Methodology, Formal analysis. **Alice Mentana:** Writing – review & editing, Writing – original draft, Visualization, Resources, Methodology, Investigation, Formal analysis. **CASTEL Rebecca:** Writing – review & editing, Writing – original draft, Visualization, Methodology, Investigation, Formal analysis. **Thierry Orsière:** Writing – review & editing, Supervision, Methodology, Conceptualization. **Stéphane Robert:** Writing – review & editing, Resources, Methodology, Formal analysis.

Declaration of Competing Interest

The authors declare that they have no known competing financial interests or personal relationships that could have appeared to influence the work reported in this paper.

Acknowledgments

The opinions and perspectives expressed are solely those of the authors and do not represent the views of the European Union. Neither the European Union nor the granting authority can be held responsible for them. The work has been carried out within the TITANS projects which received funding from the Euratom research and innovation programme 2022–2025 (grant agreement No. 101059408). The authors thanks Bernard Angeletti and the labelled Aix Marseille Platform "Elemental Chemistry" for the quantification of elemental release from particles. The authors thank the SCBM (Service de Chimie Bioorganique et de Marquage, CEA Paris-Saclay) for hosting and providing equipment, and in particular Amélie Deltheil for her technical support, and Jean-Christophe Cintrat and Frédéric Taran for their kind welcomes.

Appendix A. Supporting information

Supplementary data associated with this article can be found in the online version at doi:10.1016/j.ecoenv.2025.119491.

Data availability

Data will be made available on request.

References

Aderem, A., Underhill, D.M., 1999. Mechanisms of phagocytosis in macrophages. Annu. Rev. Immunol. 17 (1), 593–623. https://doi.org/10.1146/annurev.immunol.17.1.593.

Adeyanju, E., Okeke, C.A., 2019. Exposure effect to cement dust pollution: a mini review. SN Appl. Sci. 1 (12), 1572. https://doi.org/10.1007/s42452-019-1583-0.

Almutairi, B., Ali, D., Yaseen, K.N., Alothman, N.S., Alyami, N., Almukhlafi, H., Alakhtani, S., Alarifi, S., 2021. Mechanisms of apoptotic cell death by stainless steel nanoparticle through reactive oxygen species and Caspase-3 activities on human liver cells. Front. Mol. Biosci. 8, 729590. https://doi.org/10.3389/fmolb.2021.729590.

Badding, M.A., Fix, N.R., Antonini, J.M., Leonard, S.S., 2014. A Comparison of cytotoxicity and oxidative stress from welding fumes generated with a new nickel-, copper-based consumable versus mild and stainless steel-based welding in RAW 264.7 mouse macrophages. PLoS ONE 9 (6). https://doi.org/10.1371/journal.pone.0101310.

Baiocco, G., George, I., Garcia-Argote, S., Guardamagna, I., Lonati, L., Lamartinière, Y., Orsière, T., Rousseau, B., Ottolenghi, A., Jha, A., Lebaron-Jacobs, L., Grisolia, C., Malard, V., 2020. A 3D in vitro model of the human airway epithelium exposed to tritiated water: dosimetric estimate and cytotoxic effects. Radiat. Res. 195 (3). https://doi.org/10.1667/RADE-20-00208.1.

Bauer, M., Gräbsch, C., Gminski, R., Ollmann, A.I.H., Borm, P., Dietz, A., Herbarth, O., Wichmann, G., 2010. Cement-related particles interact with proinflammatory IL-8 chemokine from human primary oropharyngeal mucosa cells and human epithelial lung cancer cell line A549. Environ. Toxicol. 27 (5). https://doi.org/10.1002/tox.20643.

Berte, N., Eich, M., Heylmann, D., Koks, C., Van Gool, S.W., Kaina, B., 2021. Impaired DNA repair in mouse monocytes compared to macrophages and precursors. DNA Rep. 98, 103037. https://doi.org/10.1016/j.dnarep.2020.103037.

Boudjema, J., Lima, B., Grare, C., Alleman, L.Y., Rousset, D., Perdrix, E., Achour, D., Anthérieu, S., Platel, A., Nesslany, F., Leroyer, A., Nisse, C., Lo Guidice, J.-M., Garçon, G., 2021. Metal enriched quasi-ultrafine particles from stainless steel gas metal arc welding induced genetic and epigenetic alterations in BEAS-2B cells. NanoImpact 23, 100346. https://doi.org/10.1016/j.impact.2021.100346.

Butler, K.S., Peeler, D.J., Casey, B.J., Dair, B.J., Elespuru, R.K., 2015. Silver nanoparticles: correlating nanoparticle size and cellular uptake with genotoxicity. Mutagenesis 30 (4). https://doi.org/10.1093/mutage/gev020.

Cediel-Ulloa, A., Isaxon, C., Eriksson, A., Primetzhofer, D., Sortica, M.A., Haag, L., Derr, R., Hendriks, G., Löndahl, J., Gudmundsson, A., Broberg, K., Gliga, A.R., 2021. Toxicity of stainless and mild steel particles generated from gas–metal arc welding in primary human small airway epithelial cells. Sci. Rep. 11 (1). https://doi.org/10.1038/s41598-021-01177-7.

Cui, F.M., Liu, L., Zheng, L.L., Bao, G.L., Tu, Y., Sun, L., Zhu, W., Cao, J.P., Zhou, P.K., Chen, Q., He, Y.M., 2016. The role of miR-34a in tritiated water toxicity in human umbilical vein endothelial cells. Dose-Response 14 (2), 1559325816638585. https://doi.org/10.1177/1559325816638585.

Dietz, A., Ramroth, H., Urban, T., Ahrens, W., Becher, H., 2004. Exposure to cement dust, related occupational groups and laryngeal cancer risk: results of a population based case-control study. Int. J. Cancer 108 (6), 907–911. https://doi.org/10.1002/ijc.11658.

Dizdaroglu, M., Jaruga, P., 2012. Mechanisms of free radical-induced damage to DNA. Free Radic. Res. 46 (4), 382–419. https://doi.org/10.3109/10715762.2011.653969.

Dubey, K., Maurya, R., Mourya, D., Pandey, A.K., 2022. Physicochemical characterization and oxidative potential of size fractionated particulate matter: uptake, genotoxicity and mutagenicity in V-79 cells. Ecotoxicol. Environ. Saf. 247, 114205. https://doi.org/10.1016/j.ecoenv.2022.114205.

Fell, A.K.M., Nordby, K.C., 2017. Association between exposure in the cement production industry and non-malignant respiratory effects: a systematic review. BMJ Open 7 (4), e012381. https://doi.org/10.1136/bmjopen-2016-012381.

Gagnaire, B., Gosselin, I., Festarini, A., Walsh, S., Cavalié, I., Adam-Guillermin, C., Della-Vedova, C., Farrow, F., Kim, S.B., Shkarupin, A., Chen, H.Q., Beaton, D., Stuart, M., 2020. Effects of in vivo exposure to tritium: a multi-biomarker approach using the fathead minnow, Pimephales promelas. Environ. Sci. Pollut. Res. 27 (4), 3612–3623. https://doi.org/10.1007/s11356-018-3781-5.

Hartwig, A., Commission, M.A.K., 2022. Portland cement dust: MAK Value Documentation, supplement – Translation of the German version from 2020. MAK Collect. Occup. Health Saf. 7 (3). https://doi.org/10.34865/MB6599715E7_3AD.

Hill, R.L., Johnson, J.R., 1993. Metabolism and Dosimetry of Tritium. Health Phys. 65 (6), 628–647. https://doi.org/10.1097/00004032-199312000-00003.

Kain, J., Karlsson, H.L., Moller, L., 2012. DNA damage induced by micro- and nanoparticles—Interaction with FPG influences the detection of DNA oxidation in the comet assay. Mutagenesis 27 (4), 491–500. https://doi.org/10.1093/mutage/ges010.

Kelsey-Wall, A., Seaman, J.C., Jagoe, C.H., Dallas, C.E., 2006. Biological Half-Life and Oxidative Stress Effects in Mice with Low-Level, Oral Exposure to Tritium. J. Toxicol. Environ. Health Part A 69 (3), 201–213. https://doi.org/10.1080/15287390500227365.

Kodali, V., Afshari, A., Meighan, T., McKinney, W., Mazumder, M.H.H., Majumder, N., Cumpston, J.L., Leonard, H.D., Cumpston, J.B., Friend, S., Leonard, S.S., Erdely, A., Zeidler-Erdely, P.C., Hussain, S., Lee, E.G., Antonini, J.M., 2022. In vivo and in vitro toxicity of a stainless-steel aerosol generated during thermal spray coating. Arch. Toxicol. 96 (12). https://doi.org/10.1007/s00204-022-03362-7.

Krishna, L., Sampson, U., Annamala, P.T., Unni, K.M., Binukumar, B., George, A., Sreedharan, R., 2020. Genomic instability in exfoliated buccal cells among cement warehouse workers. Int. J. Occup. Environ. Med. 11 (1), 33–40. https://doi.org/10.15171/ijoem.2020.1744.

Lamartiniere, Y., Slomberg, D., Payet, M., Tassistro, V., Mentana, A., Baiocco, G., Rose, J., Lebaron-Jacobs, L., Grisolia, C., Malard, V., Orsière, T., 2022. Cyto-genotoxicity of tritiated stainless steel and cement particles in human lung cell models. Int. J. Mol. Sci. 23 (18). https://doi.org/10.3390/ijms231810398.

Lee, J.-C., Son, Y.-O., Pratheeshkumar, P., Shi, X., 2012. Oxidative stress and metal carcinogenesis. Free Radic. Biol. Med. 53 (4), 742–757. https://doi.org/10.1016/j.freeradbiomed.2012.06.002.

Leonard, S.S., Chen, B.T., Stone, S.G., Schwegler-Berry, D., Kenyon, A.J., Frazer, D., Antonini, J.M., 2010. Comparison of stainless and mild steel welding fumes in generation of reactive oxygen species. Part. Fibre Toxicol. 7 (1), 32. https://doi.org/10.1186/1743-8977-7-32.

Longhin, E., Pezzolato, E., Mantecca, P., Holme, J.A., Franzetti, A., Camatini, M., Gualtieri, M., 2013. Season linked responses to fine and quasi-ultrafine Milan PM in cultured cells. Toxicol. Vitr. 27 (2), 551–559. https://doi.org/10.1016/j.tiv.2012.10.018.

Loxham, M., Morgan-Walsh, R.J., Cooper, M.J., Blume, C., Swindle, E.J., Dennison, P.W., Howarth, P.H., Cassee, F.R., Teagle, D.A.H., Palmer, M.R., Davies, D.E., 2015. The effects on bronchial epithelial mucociliary cultures of coarse, fine, and ultrafine particulate matter from an underground railway station. Toxicol. Sci. 145 (1), 98–107. https://doi.org/10.1093/toxsci/kfv034.

Malkova, A., Svadlakova, T., Singh, A., Kolackova, M., Vankova, R., Borsky, P., Holmannova, D., Karas, A., Borska, L., Fiala, Z., 2021. In vitro assessment of the genotoxic potential of pristine graphene platelets. Nanomaterials 11 (9). https://doi.org/10.3390/nano11092210.

Matsumoto, H., Shimada, Y., Nakamura, A.J., Usami, N., Ojima, M., Kakinuma, S., Shimada, M., Sunaoshi, M., Hirayama, R., Tauchi, H., 2021. Health effects triggered

by tritium: how do we get public understanding based on scientifically supported evidence? J. Radiat. Res. 62 (4), 557–563. https://doi.org/10.1093/jrr/rrab029.
McCarrick, S., Romanovski, V., Wei, Z., Westin, E.M., Persson, K.-A., Trydell, K., Wagner, R., Odnevall, I., Hedberg, Y.S., Karlsson, H.L., 2021. Genotoxicity and inflammatory potential of stainless steel welding fume particles: an in vitro study on standard vs Cr(VI)-reduced flux-cored wires and the role of released metals. Arch. Toxicol. 95 (9). https://doi.org/10.1007/s00204-021-03116-x.
Mentana, A., Lamartinière, Y., Orsière, T., Malard, V., Payet, M., Slomberg, D., Guardamagna, I., Lonati, L., Grisolia, C., Jha, A., Lebaron-Jacobs, L., Rose, J., Ottolenghi, A., Baiocco, G., 2022. Tritiated steel micro-particles: computational dosimetry and prediction of radiation-induced DNA damage for in vitro cell culture exposures. Radiat. Res. 199 (1). https://doi.org/10.1667/RADE-22-00043.1.
Mentana, A., Orsière, T., Malard, V., Lamartiniere, Y., Grisolia, C., Tassistro, V., Iaria, O., Guardamagna, I., Lonati, L., Baiocco, G., 2023. Gaining insight into genotoxicity with the comet assay in inhomogenoeous exposure scenarios: the effects of tritiated steel and cement particles on human lung cells in an inhalation perspective. Toxicol. Vitr. 92, 105656. https://doi.org/10.1016/j.tiv.2023.105656.
Mongiat, R., Gerli, G.C., Locatelli, G.F., Fortuna, R., Petazzi, A., 1992. Erythrocyte antioxidant system and serum ceruloplasmin levels in welders. Int. Arch. Occup. Environ. Health 64 (5), 339–342. https://doi.org/10.1007/BF00379543.
OECD, 2023. Test No. 487: In Vitro Mammalian Cell Micronucleus Test. OECD. https://doi.org/10.1787/9789264264861-en.
Ogunbileje, J.O., Nawgiri, R.S., Anetor, J.I., Akinosun, O.M., Farombi, E.O., Okorodudu, A.O., 2014. Particles internalization, oxidative stress, apoptosis and pro-inflammatory cytokines in alveolar macrophages exposed to cement dust. Environ. Toxicol. Pharmacol. 37 (3). https://doi.org/10.1016/j.etap.2014.03.021.
Pandey, R.K., Prajapati, V.K., 2018. Molecular and immunological toxic effects of nanoparticles. Int. J. Biol. Macromol. 107, 1278–1293. https://doi.org/10.1016/j.ijbiomac.2017.09.110.
Panico, A., Grassi, T., Bagordo, F., Idolo, A., Serio, F., Tumolo, M.R., De Giorgi, M., Guido, M., Tutino, M., De Donno, A., 2020. Micronucleus frequency in exfoliated buccal cells of children living in an industrialized area of Apulia (Italy). Int. J. Environ. Res. Public Health 17 (4), 1208. https://doi.org/10.3390/ijerph17041208.
Patel, A., Ginhoux, F., Yona, S., 2021. Monocytes, macrophages, dendritic cells and neutrophils: an update on lifespan kinetics in health and disease. Immunology 15 (3), 250–261. https://doi.org/10.1111/imm.13320.
Pawliczak, J., Kolb, M., Bauer, M., Gminski, R., Dietz, A., Wichmann, G., 2021. Micronucleus formation in primary oropharyngeal epithelial cells reveals mutagenicity of cement dusts. Anticancer Res. 41 (4). https://doi.org/10.21873/anticanres.14951.
Platel, A., Privat, K., Talahari, S., Delobel, A., Dourdin, G., Gateau, E., Simar, S., Saleh, Y., Sotty, J., Antherieu, S., Canivet, L., Alleman, L.-Y., Perdrix, E., Garçon, G., Denayer, F.O., Lo Guidice, J.M., Nesslany, F., 2020. Study of in vitro and in vivo genotoxic effects of air pollution fine (PM2.5-0.18) and quasi-ultrafine (PM0.18) particles on lung models. Sci. Total Environ. 711, 134666. https://doi.org/10.1016/j.scitotenv.2019.134666.
Quan, Y., Tan, Z., Yang, Y., Deng, B., Mu, L., 2020. Prolonged effect associated with inflammatory response observed after exposure to low dose of tritium β-rays. Int. J. Radiat. Biol. 96 (8), 972–979. https://doi.org/10.1080/09553002.2020.1767817.
Raffetti, E., Treccani, M., Donato, F., 2019. Cement plant emissions and health effects in the general population: a systematic review. Chemosphere 218, 211–222. https://doi.org/10.1016/j.chemosphere.2018.11.088.
Rakkestad, K.E., Skaar, I., Ansteinsson, V.E., Solhaug, A., Holme, J.A., Pestka, J.J., Samuelsen, J.T., Dahlman, H.J., Hongslo, J.K., Becher, R., 2010. DNA damage and DNA damage responses in THP-1 monocytes after exposure to spores of either Stachybotrys chartarum or Aspergillus versicolor or to T-2 toxin. Toxicol. Sci. 115 (1), 140–155. https://doi.org/10.1093/toxsci/kfq045.
Roch-Lefèvre, S., Grégoire, E., Martin-Bodiot, C., Flegal, M., Fréneau, A., Blimkie, M., Bannister, L., Wyatt, H., Barquinero, J.-F., Roy, L., Benadjaoud, M., Priest, N., Jourdain, J.-R., Klokov, D., 2018. Cytogenetic damage analysis in mice chronically exposed to low-dose internal tritium beta-particle radiation. Oncotarget 9 (44), 27397–27411. https://doi.org/10.18632/oncotarget.25282.
Rose, J., Slomberg, D., Auffan, M., Payet, M., Gensdarmes, F., Malard, V., 2019. Report on production of cement particles and characterization of steel and cement suspensions (Deliverable D3.2. Transat, p. 18. ⟨https://transat-h2020.eu/resources/#1456999815432-1cdb9531-ddd0⟩ (AMU).
Santonen, T., Stockmann-Juvala, H., & Zitting, A. (2010). Review on Toxicity of Stainless Steel. Finnish Institute of Occupational Health. ⟨https://urn.fi/URN:ISBN:978-952-261-039-3⟩.
Sari-Minodier, I., Orsière, T., Auquier, P., Martin, F., Botta, A., 2007. Cytogenetic monitoring by use of the micronucleus assay among hospital workers exposed to low doses of ionizing radiation. Mutat. Res. /Genet. Toxicol. Environ. Mutagen. 629 (2), 111–121. https://doi.org/10.1016/j.mrgentox.2007.01.009.
Sari-Minodier, I., Orsière, T., Bellon, L., Pompili, J., Sapin, C., Botta, A., 2002. Cytogenetic monitoring of industrial radiographers using the micronucleus assay. Mutat. Res. /Genet. Toxicol. Environ. Mutagen. 521 (1–2), 37–46. https://doi.org/10.1016/S1383-5718(02)00213-9.
Sgambato, A., Iavicoli, I., Goracci, M., Corbi, M., Boninsegna, A., Pietroiusti, A., Cittadini, A., Bergamaschi, A., 2010. Evaluation of in vitro toxic effects of cement dusts: a preliminary study. Toxicol. Ind. Health 26 (5). https://doi.org/10.1177/0748233710365696.
Sia, J., Szmyd, R., Hau, E., Gee, H.E., 2020. Molecular mechanisms of radiation-induced cancer cell death: a primer. Front. Cell Dev. Biol. 8, 41. https://doi.org/10.3389/fcell.2020.00041.
Sotty, J., Kluza, J., De Sousa, C., Tardivel, M., Anthérieu, S., Alleman, L.-Y., Canivet, L., Perdrix, E., Loyens, A., Marchetti, P., Lo Guidice, J.-M., Garçon, G., 2020. Mitochondrial alterations triggered by repeated exposure to fine (PM2.5-0.18) and quasi-ultrafine (PM0.18) fractions of ambient particulate matter. Environ. Int. 142, 105830. https://doi.org/10.1016/j.envint.2020.105830.
Steenhof, M., Gosens, I., Strak, M., Godri, K.J., Hoek, G., Cassee, F.R., Mudway, I.S., Kelly, F.J., Harrison, R.M., Lebret, E., Brunekreef, B., Janssen, N.A., Pieters, R.H., 2011. In vitro toxicity of particulate matter (PM) collected at different sites in the Netherlands is associated with PM composition, size fraction and oxidative potential—The RAPTES project. Part. Fibre Toxicol. 8 (1), 26. https://doi.org/10.1186/1743-8977-8-26.
Turner, M.C., Krewski, D., Pope, C.A., Chen, Y., Gapstur, S.M., Thun, M.J., 2011. Long-term ambient fine particulate matter air pollution and lung cancer in a large cohort of never-smokers. Am. J. Respir. Crit. Care Med. 184 (12), 1374–1381. https://doi.org/10.1164/rccm.201106-1011OC.
Uboldi, C., Sanles Sobrido, M., Bernard, E., Tassistro, V., Herlin-Boime, N., Vrel, D., Garcia-Argote, S., Roche, S., Magdinier, F., Dinescu, G., Malard, V., Lebaron-Jacobs, L., Rose, J., Rousseau, B., Delaporte, P., Grisolia, C., Orsière, T., 2019. In vitro analysis of the effects of ITER-like tungsten nanoparticles: cytotoxicity and epigenotoxicity in BEAS-2B cells. Nanomaterials 9 (9). https://doi.org/10.3390/nano9091233.
UNSCEAR, 2017. Sources, Effects and Risks of Ionizing Radiation: 2016 Report to the General Assembly. United Nations.
Van Berlo, D., Haberzettl, P., Gerloff, K., Li, H., Scherbart, A.M., Albrecht, C., Schins, R.P.F., 2009. Investigation of the cytotoxic and proinflammatory effects of cement dusts in rat Alveolar macrophages. Chem. Res. Toxicol. 22 (9). https://doi.org/10.1021/tx900046x.
Wang, Q., Rodrigues, M.A., Repin, M., Pampou, S., Beaton-Green, L.A., Perrier, J., Garty, G., Brenner, D.J., Turner, H.C., Wilkins, R.C., 2019. Automated triage radiation biodosimetry: integrating imaging flow cytometry with high-throughput robotics to perform the cytokinesis-block micronucleus assay. Radiat. Res. 191 (4), 342. https://doi.org/10.1667/RR15243.1.
Watters, G.P., Smart, D.J., Harvey, J.S., Austin, C.A., 2009. H2AX phosphorylation as a genotoxicity endpoint. Mutat. Res. /Genet. Toxicol. Environ. Mutagen. 679 (1–2), 50–58. https://doi.org/10.1016/j.mrgentox.2009.07.007.
Westphalen, G.H., Menezes, L.M., Pra, D., Garcia, G.G., Schmitt, V.M., Henriques, J.A.P., Medina-Silva, R., 2008. In vivo determination of genotoxicity induced by metals from orthodontic appliances using micronucleus and comet assays. Genet. Mol. Res. 7 (4), 1259–1266. https://doi.org/10.4238/vol7-4gmr508.